ÇUKUROVA UNIVERSITY
INSTITUTE OF NATURAL AND APPLIED SCIENCES

MSc THESIS

Ferdi EKİNOĞLU

MODELING AND ANALYSIS OF A THREE PHASE DUAL ACTIVE BRIDGE ISOLATED BIDIRECTIONAL DC-DC CONVERTER

DEPARTMENT OF ELECTRICAL AND ELECTRONICS ENGINEERING

ADANA-2017

ÇUKUROVA UNIVERSITY
INSTITUTE OF NATURAL AND APPLIED SCIENCES

MODELING AND ANALYSIS OF A THREE PHASE DUAL ACTIVE BRIDGE ISOLATED BIRECTIONAL DC-DC CONVERTER

Ferdi EKİNOĞLU

MSc THESIS

DEPARTMENT OF ELECTRICAL AND ELECTRONICS ENGINEERING

We certify that the thesis titled above was reviewed and approved for the award of degree of the Master of Science by the board of jury on 12/12/2017.

.....	.....	.....
Asst. Prof. Dr. Adnan TAN	Assoc. Prof. Dr. M. Uğraş CUMA	Asst. Prof. Dr. M. Mustafa SAVRUN
SUPERVISOR	MEMBER	MEMBER

This MSc Thesis is written at the Department of Electrical and Electronics Engineering of Institute of Natural and Applied Sciences of Çukurova University.

Registration Number:

Prof. Dr. Mustafa GÖK
Director
Institute of Natural and Applied Sciences

ABSTRACT

MSc THESIS

MODELING AND ANALYSIS OF A THREE PHASE DUAL ACTIVE BRIDGE ISOLATED BIDIRECTIONAL DC-DC CONVERTER

Ferdi EKİNOĞLU

ÇUKUROVA UNIVERSITY
INSTITUTE OF NATURAL AND APPLIED SCIENCES
DEPARTMENT OF ELECTRICAL ELECTRONICS ENGINEERING

Supervisor : Asst. Prof. Dr. Adnan TAN
Year: 2017, Pages: 87
Jury : Asst. Prof. Dr. Adnan TAN
: Assoc. Prof. Dr. M. Uğraş CUMA
: Asst. Prof. M. Mustafa SAVRUN

High power DC-DC converters have become very important with developments in especially electric vehicle, renewable energy conversion, aerospace, and railway applications. Most of these applications require DC-DC conversion stages that are also very important for the system efficiency. Since the energy conversion takes place at high power levels in these applications, DC-DC converter stages are very effective for the system efficiency and stability. In addition, bidirectional energy transfer and low weight requirements are common issues for most of these applications. This fact requires some considerations and system improvement activities to provide more stable and efficient systems. The dual active bridge (DAB) topology is one of the effective topology that contributes to overcome these problems. Dual active switching elements are used to provide bidirectional power transfer and high frequency isolation transformer is used to provide low weight system design. In this thesis a three phase dual active bridge isolated bidirectional DC-DC converter is modeled and analyzed. The input voltage is determined as 600 V the output voltage is determined as 800 V and the system nominal power is determined as 80 kW. The Input and the output voltages and the power range are determined based on railway operating ranges. Unstable conditions of voltage and the load are also considered in this system design.

Key Words: Dual-Active Bridge, DC-DC Converter, Phase Shift, High Power Converter

ÖZ

YÜKSEK LİSANS TEZİ

ÜÇ FAZ ÇİFT AKTİF KÖPRÜLÜ İZOLELİ İKİ YÖNLÜ DA-DA DÖNÜŞTÜRÜCÜNÜN MODELLENMESİ VE ANALİZ EDİLMESİ

Ferdi EKİNOĞLU

ÇUKUROVA ÜNİVERSİTESİ
FEN BİLİMLERİ ENSTİTÜSÜ
ELEKTRİK ELEKTRONİK MÜHENDİSLİĞİ ANABİLİM DALI

Danışman : Yrd. Doç. Dr. Adnan TAN
Year: 2017, Pages: 87
Jüri : Yrd. Doç. Dr. Adnan TAN
: Doç. Dr. M. Uğraş CUMA
: Yrd. Doç. Dr. Murat Mustafa SAVRUN

Yüksek güçlü DC-DC dönüştürücüler özellikle elektrikli araç, yenilenebilir enerji dönüşümü, uzay ve demiryolu uygulamaları alanındaki gelişmelerle birlikte çok önemli hale gelmiştir. Bu uygulamaların çoğu, sistem verimliliği için çok önemli olan DC-DC dönüştürme aşamalarını gerektirir. Enerji dönüşüm bu uygulamalarda yüksek güç seviyelerinde gerçekleştiğinden, DC-DC dönüştürücü aşamaları sistem verimliliği ve kararlılığı için çok etkilidir. Buna ek olarak, çift yönlü enerji aktarımı ve düşük ağırlık gereksinimleri, bu uygulamaların çoğunda yaygın olan konulardır. Bu gerçek, daha istikrarlı ve verimli sistemler sağlamak için bazı hususlar ve sistem iyileştirme faaliyetleri gerektirir. Çift yönlü aktif köprü (ÇYAK) topolojisi bu sorunların üstesinden gelmeye katkıda bulunan etkili topolojilerden biridir. Çift aktif anahtarlama elemanları çift yönlü güç aktarımını sağlanmak, yüksek frekanslı izolasyon transformatörü ise düşük ağırlıklı sistem tasarımı sağlamak için kullanılmaktadır. Bu tezde üç faz aktif köprülü izoleli iki yönlü DA-DA dönüştürücü modellenmiş ve analiz edilmiştir. Giriş voltajı 600 V, çıkış voltajı 800V, sistem nominal gücü 80 kW olarak belirlenmiştir. Giriş ve çıkış voltajları ve güç aralığı demiryolu çalışma aralıkları baz alınarak belirlenmiştir. Bu sistem tasarımında kararsız gerilim ve yük koşulları da göz önüne alınmıştır.

Anahtar Kelimeler: Çift Yönlü Aktif Köprü, DA-DA Dönüştürücü, Faz Kaydırma, Yüksek Güçlü Dönüştürücü

EXTENDED SUMMARY

In the last decade, some electric applications such as renewable power conversion, electric vehicle, railway, charging, have become very popular with the threat of energy shortage that is still increasing. Some of these applications require auxiliary power supplies or high power energy conversions. Since all of these applications and their conversion stages take place under high power levels, high power DC-DC conversions has become very important.

Various bidirectional isolated dc-dc converters have been proposed as a solution for high power applications. Most of the presented dc-dc converters have asymmetrical circuit configurations to couple the two dc links having largely different voltages, several tens volts and several hundred volts (Chiu et al., 2006; Inoue et al., 2007).

Every energy conversion system has some losses that depend on some parameters. The selection of correct topology and parameters directly affects the efficiency of the circuit and it is very important for such a system. Selecting of the right topology is also depends on a few parameters such as power density level, working conditions, permissible space for circuit, power flow direction. Since high power applications such as railway, charging and discharging of high power energy storage devices are also requires high-efficiency power converters, high-frequency-link (HFL) power conversion systems (PCSs) are attracting more and more attentions in academia and industry due to reduced weight, and low noise without compromising efficiency, cost, and reliability (Tan et al., 2012;Zhao et al., 2014). Due to the importance of safety, weight and free space limitations in some high power applications, it is very important to use an effective topology that provides safety and compact design for the system.

The dual active bridge converter, has been shown to be an attractive alternative for high-power applications (De Donker et al, 1991). In the converter

active devices on both the input and output sides are used to realize an optimal topology that has low device stresses (Kheraluwala et al., 1992).

Based on high power application requirements, in this thesis a 80 kW three phase dual active bridge isolated bidirectional DC-DC converter operates with 600 V input and 800 V output voltages, is modeled and its operating conditions are analyzed. A small size and a low cost high frequency transformer is used in the DC-DC converter to provide isolation. Some DC-DC converter topologies, and various modulation strategies are also discussed. Based on high power applications, different topologies and modulation strategies are compared and the key factors of selection optimal topology are discussed. This selection is supported with the simulation results. An effective measurement and controller systems are designed to overcome voltage and load fluctation problems in high power applications.

MATLAB/Simulink program is used for the simulation analysis. This program is an effective solution to analysis the circuit with the parameters that provides get results close to the reality.

.

ACKNOWLEDGEMENTS

I would like to express my heartfelt thanks to my supervisor Asst. Prof. Dr. Adnan TAN for his supervision, guidance, encouragements and extremely useful suggestions throughout this thesis. It has been a great honor to have Asst. Prof. Dr. M. Adnan TAN as supervisor.

I would like to thank Asst. Prof. Dr. M. Uğraş Cuma for his extremely valuable guidance and suggestions throughout in the thesis. His technical assistance and personal advice have been invaluable.

I would also like to thank you to Asst. Prof Dr. Murat Mustafa Savrun and Tahsin Köroğlu for their valuable advices and strong technical support. Their continuous support helped me to finish this thesis.

I wish also to extend my acknowledgements to all staff members in the department and my friends.

Ferdi EKİNOĞLU

CONTENTS **PAGE**

LIST OF TABLES **PAGE**

LIST OF FIGURES **PAGE**

LIST OF SYMBOLS

I_i	:	Supply Current
I_o	:	Load Current
i_i	:	Input Side DC Link Current
i_o	:	Output Side DC Link Current
i_{Ci}	:	Input Side DC Link Capacitor Current
i_{Co}	:	Input Side DC Capacitor Current
C_i	:	Input Side DC Link Capacitor
C_o	:	Output Side DC Link Capacitor
Vi	:	Input DC Voltage
Vo	:	Output DC Voltage
L	:	Total Equivalent Inductance
L_1	:	Primary Serial Inductance
i_p	:	Single Phase Transformer Primary AC Current
i_s	:	Single Phase Transformer Secondary AC Current
v_p	:	Single Phase Transformer Primary AC Voltage
v_s	:	Single Phase Transformer Secondary AC Voltage
v'_s	:	Primary Referred of vs
i'_o	:	Primary Refered of i_o
V'o	:	Primary Referred of Vo
ø	:	Phase Shift Angle
T1,2,3…8	:	IGBTs
i_{ap}	:	Three Phase Transformer Primary AC Current
i_{as}	:	Three Phase Transformer Secondary AC Current
v_{ap}	:	Transformer Phase-a Primary to Neutral Voltage
v_{as}	:	Transformer Phase-a Secondary to Neutral Voltage
v'_{as}	:	Primary Referred of v'_{as}

f_{sw}	:	Switching Frequency
ω	:	Angular Frequency
D	:	Duty Cycle
d	:	V_o/V_i

LIST OF ABBREVATIONS

DC	: Direct Current
DAB	: Dual Avtive Bridge
SPDAB	: Single Phase Dual Active Bridge
TPDAB	: Three Phase Dual Active Bridge
HFL	: High Frequency Link
PCS	: Power Conversion System
ZVS	: Zero Voltage Switching
HFT	: High Frequency Transformer
AC	: Alternative Current
RMS	: Root Mean Square
PWM	: Pulse Width Modulation
IGBT	: Insulated Gate Bipolar Transistor
IEEE	: The Institute of Electrical and Electronics Engineers
UPS	:Uninteruptable Power Supply

1. INTRODUCTION

1.1. General Overview of DC-DC Converters

A lot of topologies have been proposed for DC to DC converters in the literatures. All topologies have their own advantages and disadvantages depend on suitability of the application. Figure 1.1 shows the general list of common used DC-DC converters.

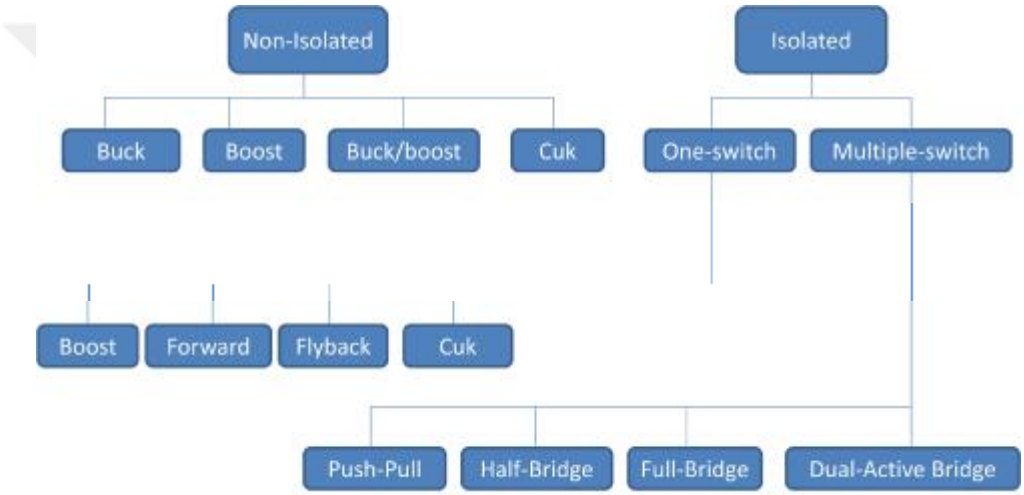

Figure 1.1. General list of common used DC-DC converters

Buck converter is the simplest type of converters. It is used when the required output voltage is smaller than the input voltage. It also uses small number of components and the losses are very small. Boost converter topology is similar to the buck converter topology as component number and simplicity however in boost converter, the output voltage is higher than the input voltage. Both of these topologies contain at least one diode and transistor and also one energy storage element such as capacitor. Buck-boost converter is a combined form of buck and boost topologies. It provides higher or lower output voltage respect to input voltage and the output voltage polarity change also possible with this topology with respect

to the common terminal of the input current. Containing small number components and the simplicity are the advantages of these converters however high input voltage ripples and the electrical stresses are disadvantages of these converters. Figure 1.2 shows the basic buck, boost and buck-boost circuits. (Yilmaz et al.; 2013)

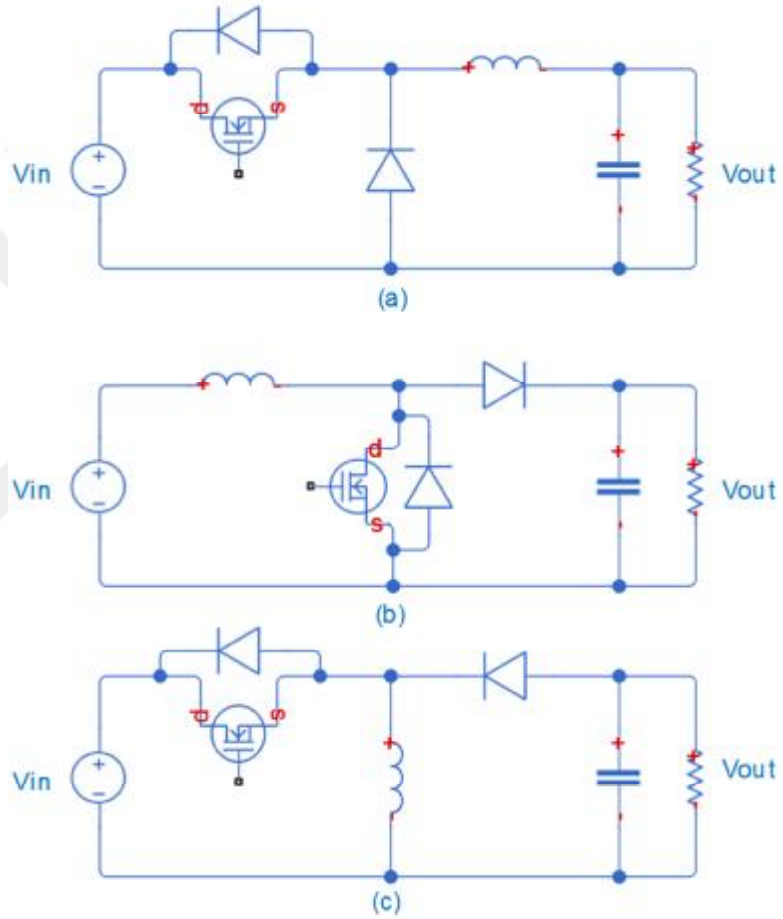

Figure 1.2. Buck (a), boost (b), buck-boost converter circuits

When the isolation is required in applications flyback converter can be an alternative for low power ranges. The flyback converter does not contain any inductor at the output side thus it is possible to obtain high output voltages. This

converter is also low-cost and simple, however high electrical stresses and lower efficiency due to leakage inductance, are disadvantages of the flyback converter. Figure 1.3 shows the basic flyback converter circuit. (Yilmaz et al.; 2013)

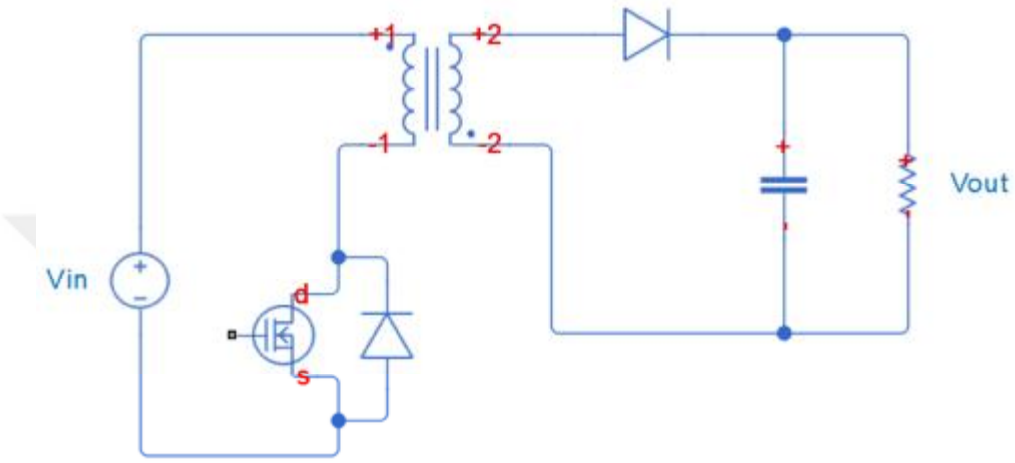

Figure 1.3. Basic flyback converter circuit

Forward converter is a transformer-isolated converter based on basic buck converter topology (Microchip, 2007). The advantages of these converter are low input capacitor ripple current, lower current on the secondary side diodes and simplicity (Yilmaz et al., 2013). Higher transistor rating, requirement of active snubber circuit and higher conduction losses are disadvantages of this converter. Figure 1.4 shows the basic forward converter circuit.

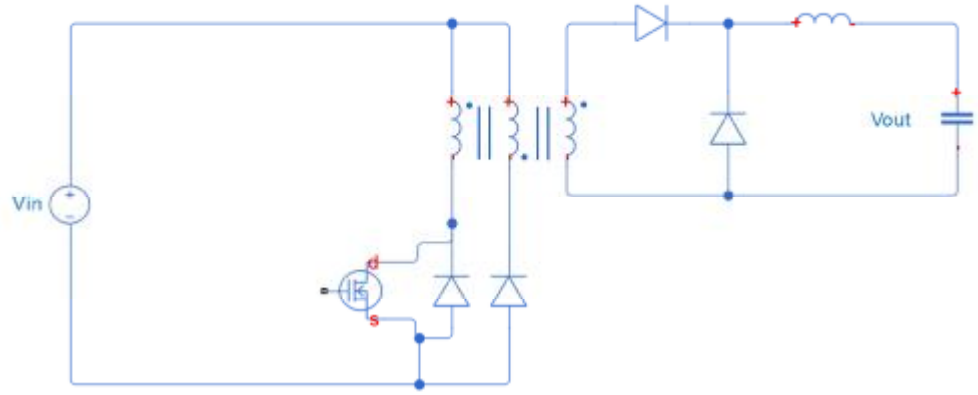

Figure 1.4. Basic forward converter circuit

Push-pull converter is another transformer-isolated converter based on the basic forward topology (Microchip, 2007). Comparing with previous converters shows that higher power levels can be achieved with this topology. Figure 1.5 shows basic push-pull converter circuit.

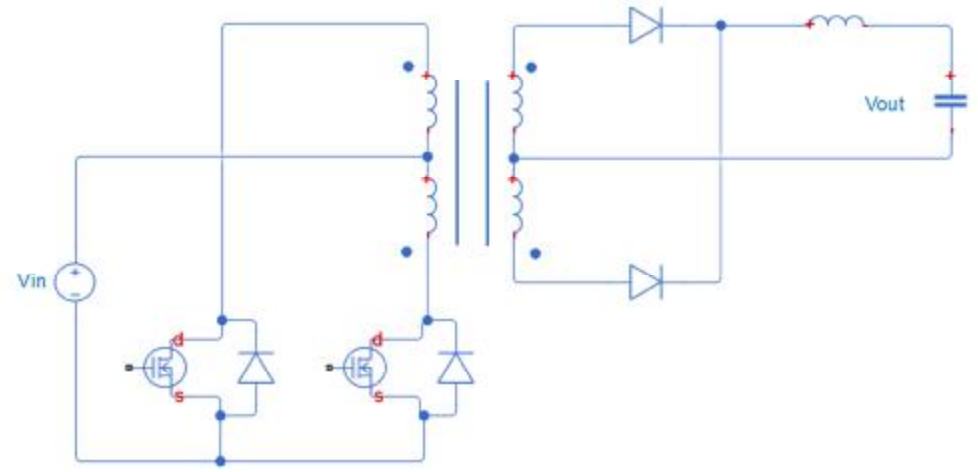

Figure 1.5. Basic push-pull converter circuit

Similar to the buck-boost topology, it is possible to obtain a negative polarity output voltage with respect to the common terminal of the input with CUK converter. This converter provides reduced continuous input and output current however it requires high number of passive components and large inductors. High

electrical stress is also another disadvantage of this converter (Yilmaz et al., 2013). Figure 1.6 shows the basic circuit of the CUK converter.

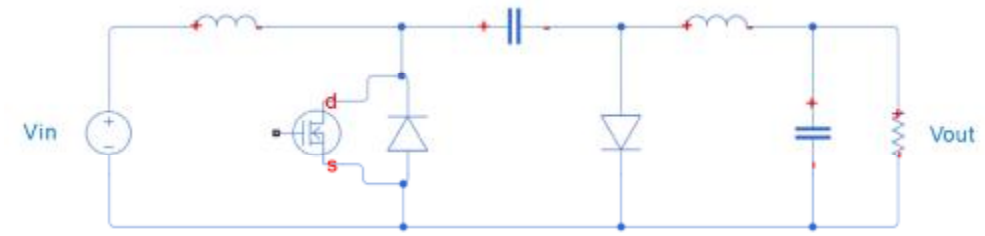

Figure 1.6. Basic CUK converter circuit

SEPIC converter is consists of two large inductors, switching component, diode and capacitors. Unlike the CUK converter the output current is discontinuous and it has a non-inverting buck-boost characteristic. The CUK and the SEPIC converters can be operated as bidirectional converter by using two active switches. However the current stress for semiconductor components, is higher than the other bidirectional converters (Yilmaz et al., 2013). Figure 1.7 shows the basic circuit of SEPIC converter.

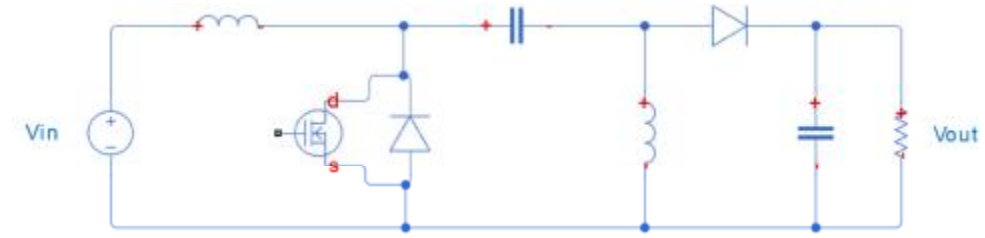

Figure 1.7. Basic SEPIC converter circuit

Half-bridge converter is a transformer-isolated converter based on basic forward converter (Microchip, 2007). It contains small number of components and requires simple control strategy. It is a low cost converter however it has high component stress. Comparing with the CUK and SEPIC converters, half-bridge converter provides higher efficiency since it has lower inductor conduction and

switching losses. The major drawback of this topology is discontinuous output current when operating as boost (Yilmaz et al., 2013). Figure 1.8 shows the basic circuit of half-bridge converter.

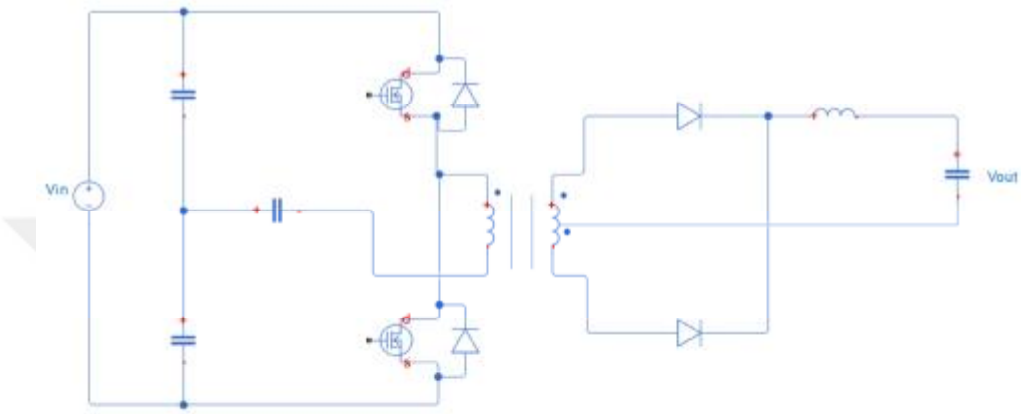

Figure 1.8. Basic half-bridge converter circuit

Full-bridge converter is a transformer-isolated buck converter (Microchip, 2007). It contains more component numbers and requires more complex control strategy. Thus it is a higher cost converter. However it provides a high conversion ratio, high power level and low component stress (Yilmaz et al., 2013). The full-bridge topology is an effective solution for higher power levels. The Figure 1.9, which will be defined as Topology A in the following chapter, shows the basic circuit of the full bridge converter. It contains controlled device on the first side, and uncontrolled diodes on the second side and the galvanic isolation between two sides. Operation in constant frequency, allows optimum design of magnetic and filter components, minimum voltage-ampere stresses, good control range and controllability are some advantages of this topology. However it has some limitations based on switching losses with increasing frequency and high voltage stress is induced by the parasitic inductances following diode reverse recovery (Kheraluwala et al., 1991).

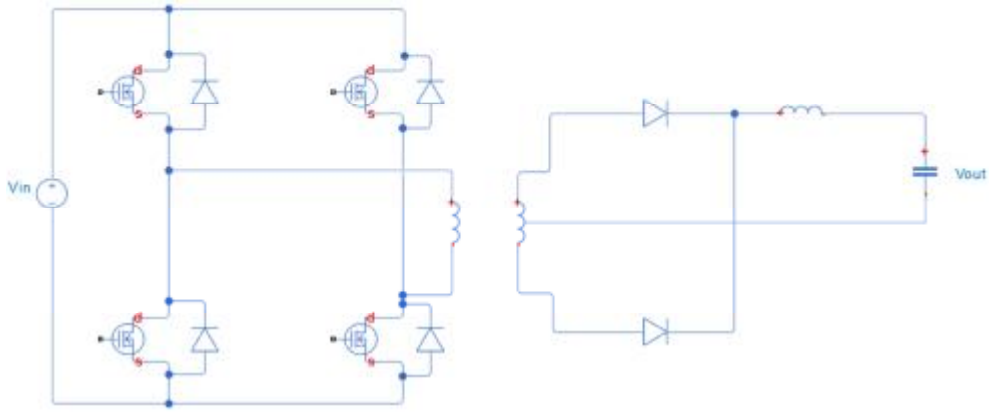

Figure 1.9. Basic full-bridge converter circuit

There are also some advanced topologies that provides more efficient system design using zero voltage and zero current switches based on snubber circuit and resonant network. Resonant dc/dc converters, quasi-resonant dc/dc converters, multi-resonant dc/dc converters and the quasi-square wave converters are main soft switching topologies in the literature (Kheraluwala et al., 1991). These topologies require detailed calculations and complex control circuit design.

1.2. High Power DC-DC Converter Topologies

The field of high-power density dc-to-dc has received a lot of attention in recent years (Kheraluwala et al., 1992). These converters are used in various applications mainly automotive, aerospace, renewable energy power systems, battery charging and auxiliary power supply units for light rail vehicles.

The buck, boost, buck-boost, flyback, forward, push-pull, SEPIC and CUK converters are not sufficient for high power levels. Some of these topologies have extended variations to provide operating higher power levels however, these topologies are more complex and their power levels are also not sufficient enough.

Three DC-DC converter topologies are presented which are used for high power density applications will be discussed. In these topologies full bridge

method is used for minimum device stresses, constant frequency operation is used for efficient transformer and filter and controller design (Kheraluwala et al., 1991).

1.2.1. Topology A Single-Phase Single Active Bridge DC-DC Converter (Full Bridge)

In this section the full-bridge converter topology is defined as Topology A (Kheraluwala et al., 1991). Figure 1.10 shows the basic circuit block scheme of the Topology A. This circuit was derived from some older topologies by applying a modification. The output filter inductor has been transferred to the ac side (in effect lumping it with the transformer leakage inductance). This modification allows energy storage in leakage inductance and lossless manner transfer to the load. Also, it allows controlling soft-switching conditions with this sole effective leakage inductance. Power flow is controlled by the applying phase shift between two resonant poles of the input bridge.

The dual active bridge converter is an alternative solution that allows operation in high power levels and bidirectional power transfer. This converter offers easier control strategy than other high power converters such as multilevel. Single and three phase topologies are possible for the dual active bridge converter.

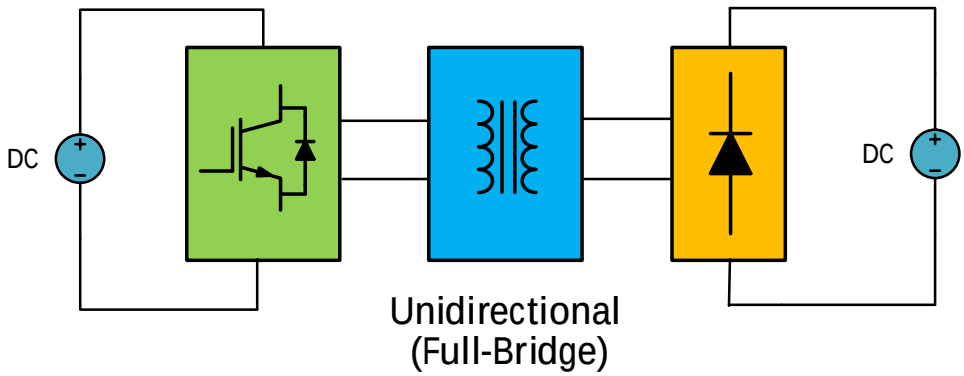

Figure 1.10. Topology A circuit block scheme

1.2.2. Topology B Single-Phase Dual Active Bridge (DAB) DC-DC Converter

Since the secondary side circuit of Topology A consist of uncontrolled diodes, it is not possible to provide bi-directional power flow. Replacing the diodes with active devices allows controlling bidirectional power flow and also simpler control strategy of handling diode recovery process as shown in Figure 1.11 (Kheraluwala et al., 1991)

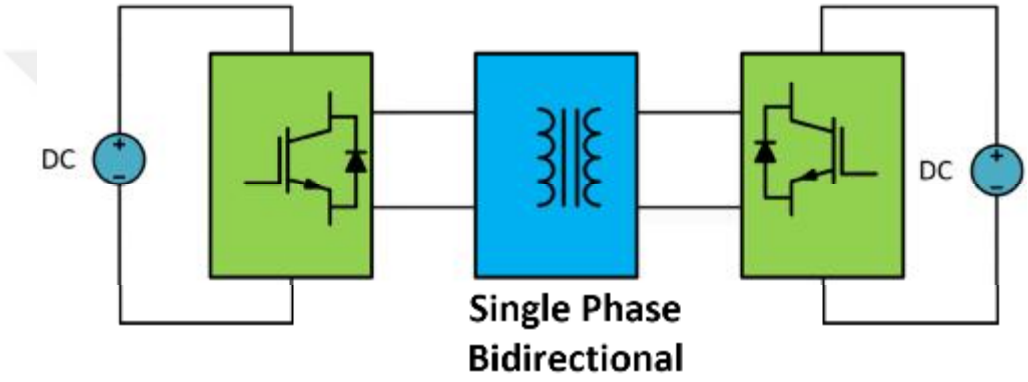

Figure 1.11. Topology B circuit block scheme

1.2.3. Topology C Three-Phase Dual Active Bridge (DAB) DC/DC Converter

Topology C is a three phase extension of Topology B (Kheraluwala, 1991). As shown in the Figure 1.12. The three-phase legs of each bridge are operated with a phase shift of 120^{o} (Hoek et al., 2013). Although both Topology B and Topology C could be used for higher power requirements, there are some performance and power quality differences between them. These differences will be discussed in following chapter.

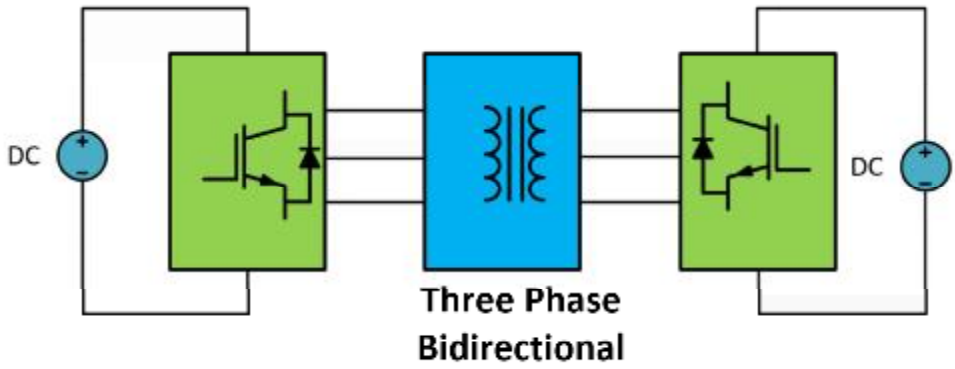

Figure 1.12. Topology C circuit block scheme

1.3. Motivation of Thesis

Many modern power conversion systems require not only unidirectional but also bi-directional energy transfer capability. Preferably, such systems should use a single high efficiency power electronic conversion system to reduce the size, the weight and the cost (Segaran et al., 2008). For higher power requirements the common used structure is the bidirectional dual active bridge topology.

The dual active bridge topology is used in vary applications such as uninterruptable power supply (UPS), renewable generation systems, energy storage systems, smart grid, automotive and motor drive systems, with the regeneration capability and the multilevel conversion systems.

The dual active bridge topology presents an alternative solution for the classical full bridge topology problems. Moving output inductor to the AC side as series to the transformer leakage inductance, prevents the reverse recovery losses in the output diodes. This allows higher switching frequencies and, therefore, an increase in the power density. Furthermore, the use of an active output bridge also increases the power density of the transformer. As a result of all these benefits, low device stress, small filters, high transformer utilization and low-switching losses are provided by this topology (Baars et al., 2015).

Due to all these advantages, the dual active bridge topology is the one of the most suitable topology for high power DC DC converters. Despite its benefits and advantages there are no sufficient researches on literature.

1.4. Scope and Objectives of the Thesis

In this thesis a three phase dual active bridge isolated bidirectional DC-DC converter is designed and implemented as operating with 600 V input, 800 V output voltages and providing 80 kW output power. The simulation of this converter also implemented based on high power applications. Two three phase converters are connected via an isolated transformer and an inductor that is used as power transfer element. Insulated gate bipolar transistors (IGBTs) are selected as switching device and six IGBTs are used for each side of converter. 20 kHz switching frequency is applied to the IGBTs. Positive or negative phase shift is applied to provide bidirectional power flow.

This converter is simulated using MATLAB/Simulink program. To achieve a realistic simulation analysis, the parameters of power circuit devices are set with the specifications of real components.

The performance of modeled system is analyzed and verified with various different case studies. In addition, the efficiency of the system is investigated in different load conditions.

1.5. Outline of the Thesis

The overall structure of the thesis is as follows:

In Chapter 1, the high power DC-DC converters are introduced. Different DC-DC converter topologies and their advantages and disadvantages are discussed. Motivation and the purpose of the thesis are also summarized.

In Chapter 2, dual active bridge DC-DC converter topologies circuit diagrams and ideal operation waveforms of these converters are discussed. Single phase and three phase systems are compared.

In Chapter 3, the modeling studies of the three phase dual active bridge converter design is presented. Design considerations, selection of components, switching conditions and the calculations are explained. The way of implementation of these circuits in MATLAB/Simulink is also presented.

In Chapter 4, some different operating and load conditions are analyzed as case studies and the results are interpreted.

In Chapter 5, all the thesis subjects are summarized and the results of the Chapter 4 are interpreted.

In Chapter 6, future works are summarized.

2. OPERATING PRONCIPLES OF DAB CONVERTERS

The DAB converter was first developed in the University of Wisconsin Madison in 1989. Since then the converter has gained popularity because of its high power density, high efficiency due to zero voltage switching (ZVS) operation under wide load range, bidirectional operation and high frequency isolation (Dutta et al., 2014). Either single-phase or three-phase converters have been proposed for such a system, but to date no clear-cut basis for selecting between these two alternatives has been established (Segaran et al., 2008). Single-phase and three-phase DAB topologies are discusses and compared in the next chapters. The bidirectional converter structure consists of two unidirectional DC-DC converters as shown in the Figure 2.1

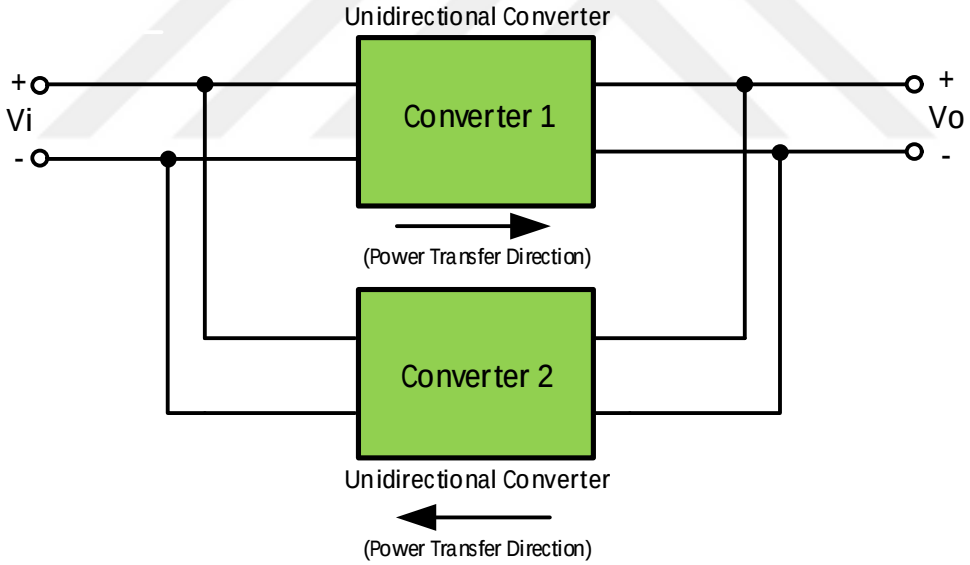

Figure 2.1. The principle construction of bidirectional converterIi

2.1. Single Phase Dual Active Bridge DC-DC Converter

Single phase dual active bridge (SPDAB) DC-DC converters consist of two DC sources, eight active switching devices, input and output filters, and a high frequency isolation transformer.

2.1.1. The Circuit of SPDAB DC-DC Converter

The basic of SPDAB DC-DC converter circuit is presented in the Figure 2.2. As shown in the figure, the SPDAB topology consists of two seperate converters coupled via an isolation transformer and a series inductor. It is better to transform the circuit as primary-referred as in the Figure 2.3, to take into account transformer leakage inductance. L is the total inductance referred to the primary side.

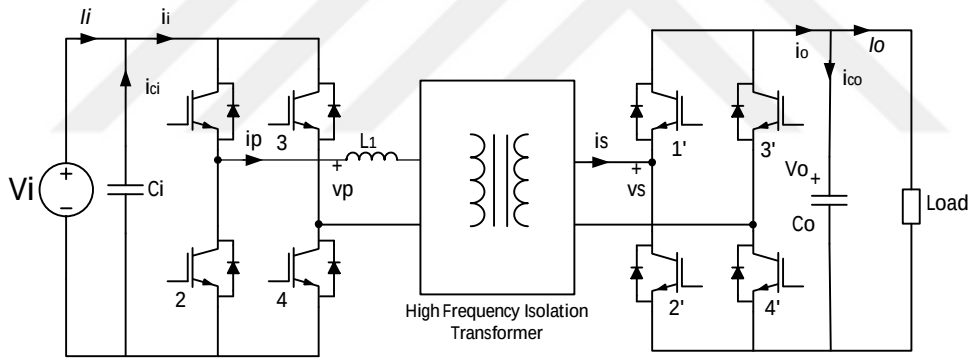

Figure 2.2. SPDAB circuit scheme

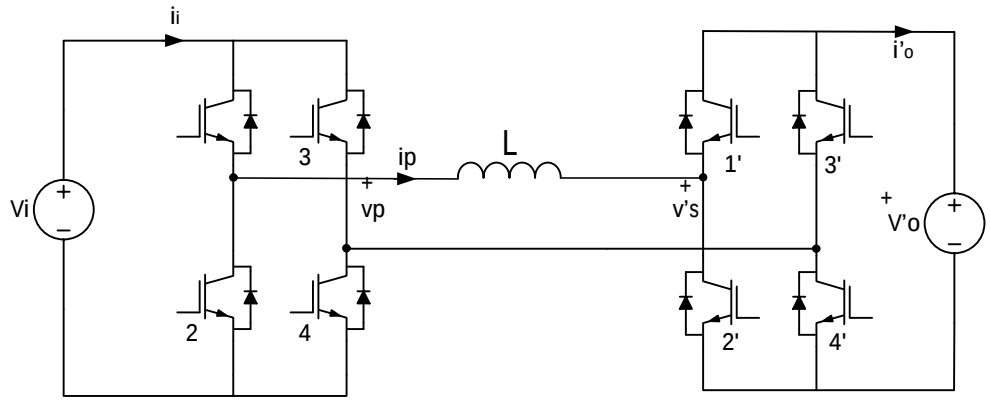

Figure 2.3. Primary referred equivalent circuit of SPDAB

2.1.2. The Operation of SPDAB DC-DC Converter

Regarding primary referred circuit of SPDAB, the circuit can also be derived as two AC source are interconnected with series inductor as shown in the Figure 2.3. Considering the circuit as in the Figure 2.3, the AC sources are controlled to regulate real and reactive power flow by varying magnitude and phase relationship. In normal operation the required reactive power for inductor is supplied by either one or both of the AC sources depending on their relative voltage magnitudes. Magnitude differences between v_p and the v'_s voltages, causes additional reactive power circulation between the two sources this will require increased current more than necessary to transfer the required real power, and this causes increasing of losses. This must be considered while deciding the transformer turns ratio (Segaran et al., 2008).

There are some issues which should be considered for switching strategy. Recognizing the circuit as in the Figure 2.4 as dual converter system is only possible if both converters are PWM modulated to produce AC fundamental output. However this approach has some limitations on switching frequency. For converters, the ratio of PWM and the fundamental AC frequency should be at least 9 for acceptable harmonic performance of the PWM. As practical for high power converters the maximum switching frequency is limited perhaps 50 kHz.

According to this ratio the AC fundamental frequency is limited around 5 kHz. This low fundamental frequency limits using ferrite cores for designing the isolation transformer and the inductor (Segaran et al., 2008).

Figure 2.4. The derivative equivalent circuit of SPDAB (Segaran et al., 2008)

Another approach to face this problem is, square-wave modulation for both converters of the dual-active system. Real-power flow is provided by applying phase shift between two converters (Segaran et al., 2008). Figure 2.5 and Figure 2.6 show the power flow directions regarding the applied phase shift angle “ø” between two converters.

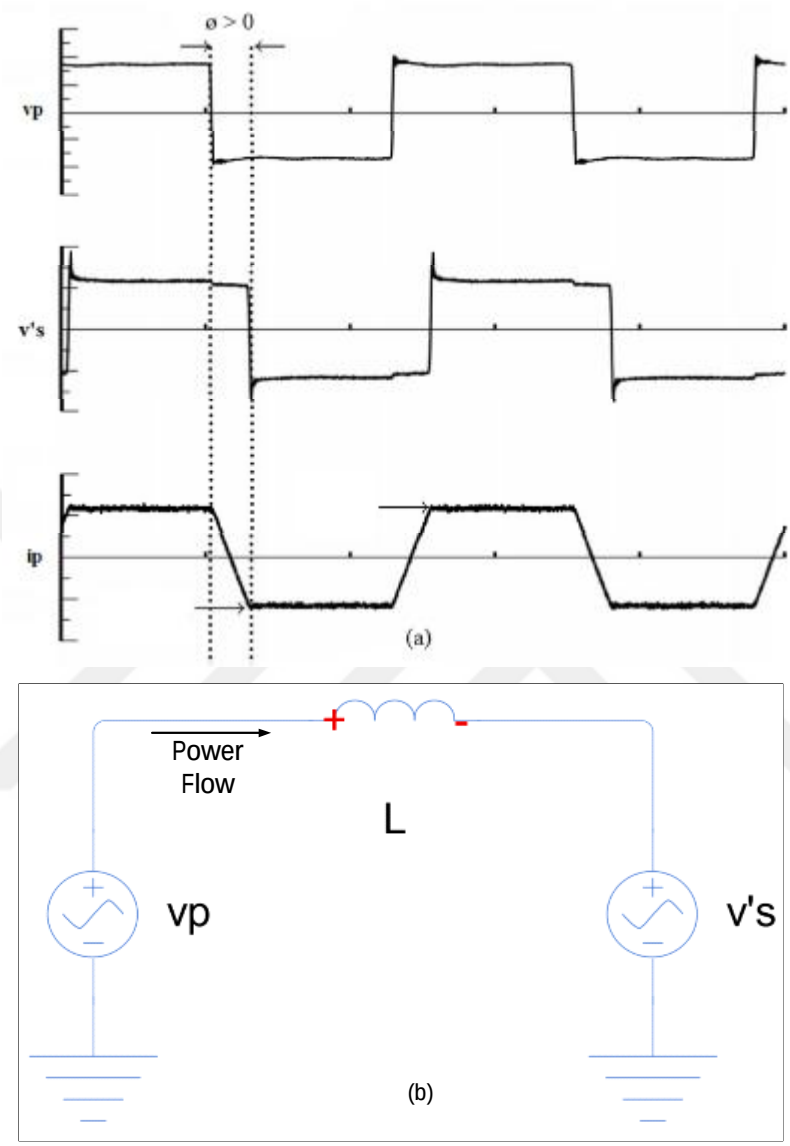

Figure 2.5. Waveforms (a) and power flow direction (b) with applied positive phase shift

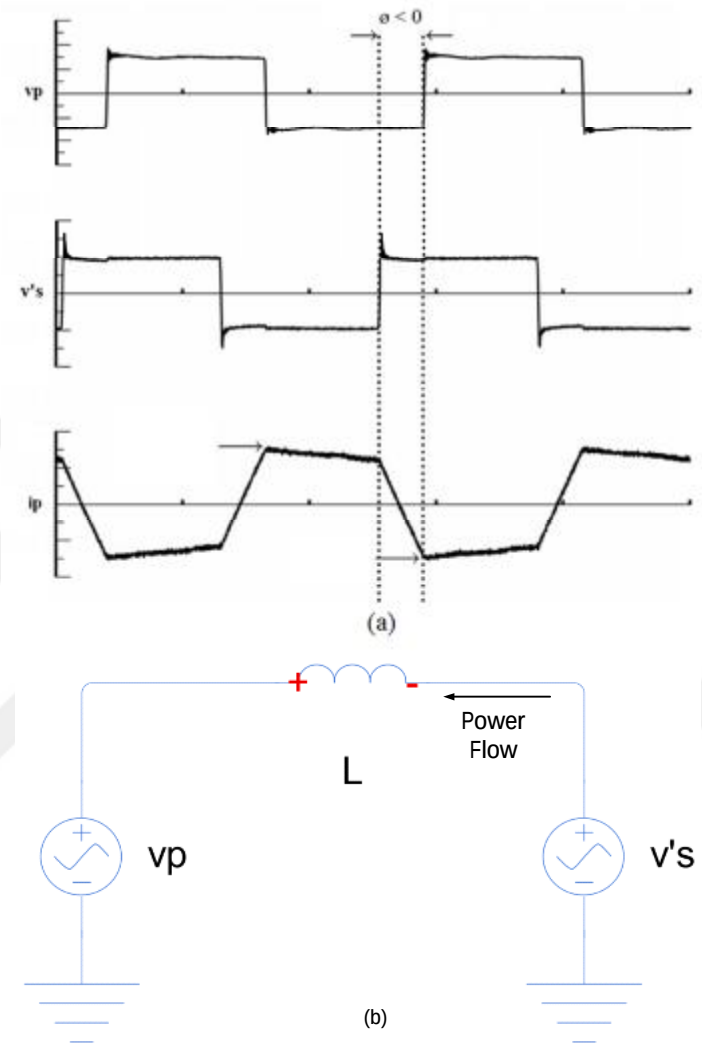

Figure 2.6. Waveforms (a) and power flow direction (b) with applied negative phase shift

Figure 2.7 also shows the idealized waveforms of the phase shift modulation for the SPDAB regarding the circuit in the Figure 2.2. As shown in the Figure 2.7, three possible current waveforms are illustrated regarding the magnitude difference consideration of both Vi and V'o. 180^{o} phase shift is applied between the two switching devices which are in the same phase leg (such as T1 and

T2 or T2 and T4). The phase shift is also applied between the each side of the converter.

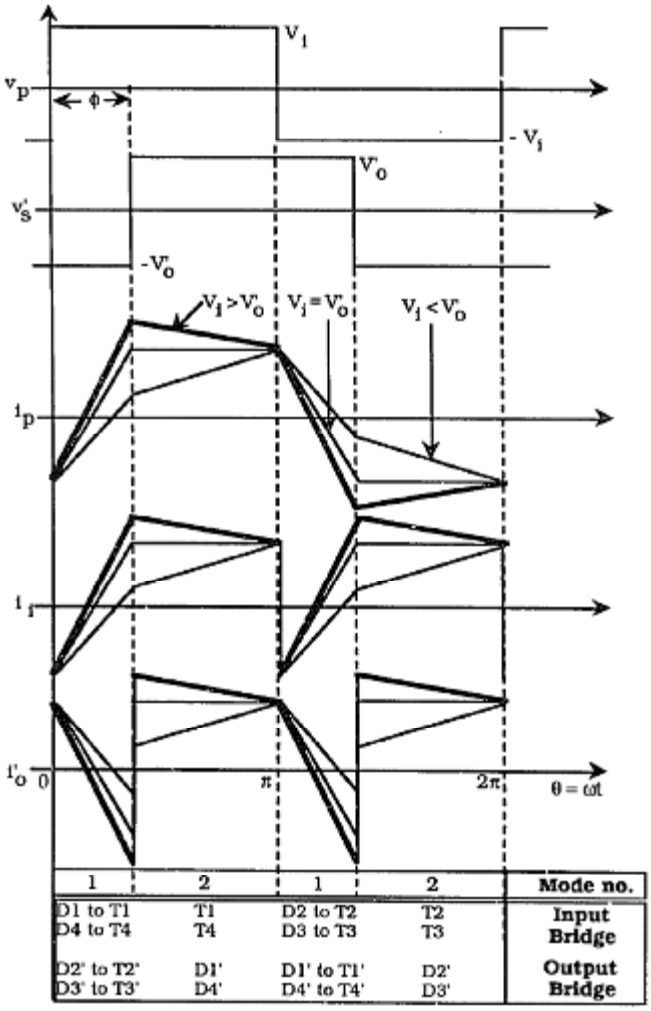

Figure 2.7. Idealized waveforms of phase shift modulation for SPDAB (Kheraluwala et al., 1991)

2.2. The Circuit of TPDAB DC-DC Converter

The circuit of TPDAB is basically shown in the Figure 2.8. As shown in the figure it consists of two separate three phase active bridge converters and each phase are connected via series inductors and an isolation transformer. As mentioned before the circuit designs and the basics are similar for both single and three phase DAB system but the design considerations are different.

2.2.1. The Operation of TPDAB DC-DC Converter

The operation of TPDAB converters is simply three phase derivation of the SPDAB converters. The six active switching devices for each bridge operate in six-step mode at a fixed frequency. The power flow is provided by applying a phase shift between two sides of the converter (Kheraluwala et al., 1991). The other considerations are also valid for this three phase system. The primary equivalent circuit diagram of TPDAB converter is also shown in Figure 2.9.

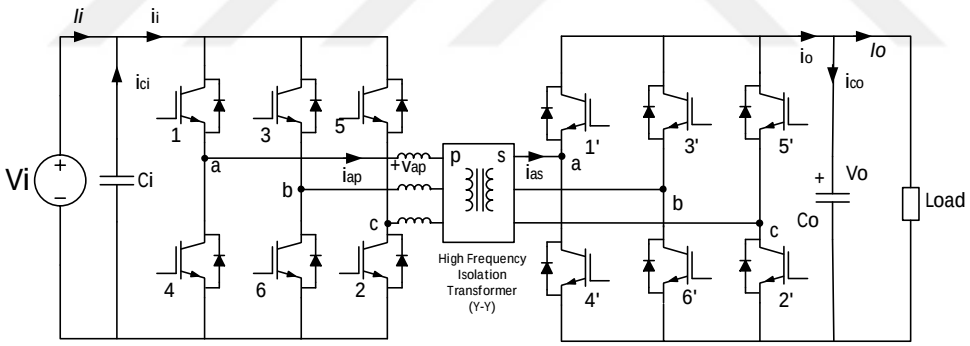

Figure 2.8. The basic circuit scheme of TPDAB converter

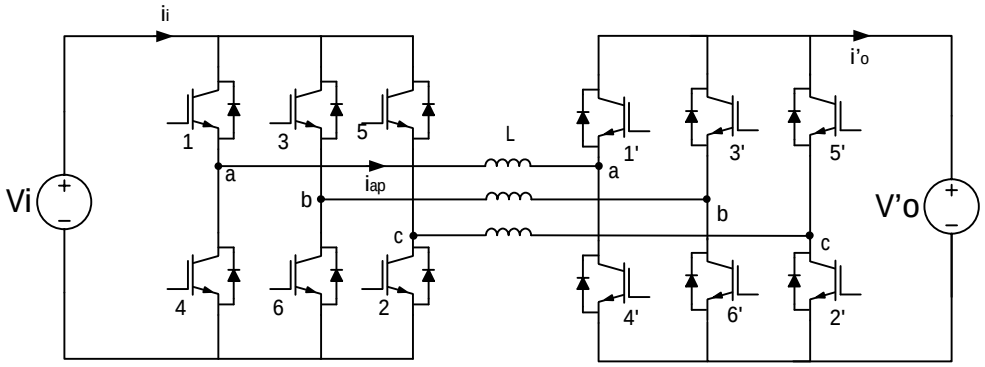

Figure 2.9. The primary referred equivalent circuit diagram of TPDAB converter

There are two possible distinct interval for the phase shift angle "ø"

- Region I: $0 \leq \text{ø} < \pi/3$
- Region II: $\pi/3 \leq \text{ø} < \pi/2$

There are also six modes operation in each region. In each mode i_{ap} is a function of $\theta = \omega t$, where ω is $2\pi f_{sw}$ and f_{sw} switching frequency, is given by,

$$iap(\theta) = \frac{[Vap(\theta) - Vas'(\theta)}{\omega L}(\theta - \theta i) + iap(\theta i) \qquad \theta_i \leq \theta \leq \theta_f \qquad (2.1)$$

Where the θ_i and the θ_f is the start and the end of the each mode respectively, v_{ap} is the Phase-a primary to neutral voltage, v'_{as} is the Phase-a secondary voltage referred to the primary side and $i_{ap}(\theta_i)$ is the I ünitial current of each mode. Regarding the transformer connected as Y-Y, the entire analyis is presented below based on region I an region II. Figure 2.10 and 2.11 also shows the conduction sequences and waveforms according to these regions. The input bridges leads the output bridge (for $\text{ø} \geq 0$) and analysis for reverse power flow ($\text{ø} \leq 0$) is identical (Kheraluwala et al., 1991).

Region I

· Mode 1 : $0 \leq \theta < ø$; $v_{ap}(\theta)=Vi/3$; $v_{as}'(\theta)= -V_o'/3$

$$iap(\theta)=\frac{Vi+Vo'}{3\omega L}(\theta) + iap(0) \quad (2.2)$$

· Mode 2 : $ø \leq \theta < \pi/3$; $v_{ap}(\theta)=V_i/3$; $v_{as}'(\theta)= V_o'/3$

$$iap=\frac{(Vi-Vo')}{3\omega L}(\theta - ø) + iap(ø) \quad (2.3)$$

· Mode 3 : $\pi/3 \leq \theta < (ø+\pi/3)$; $v_{ap}(\theta)=2V_i/3$; $v_{as}'(\theta)= V_o'/3$

$$iap=\frac{(2Vi-Vo')}{3\omega L}(\theta - \pi/3) + iap(\pi/3) \quad (2.4)$$

· Mode 4 : $(ø+\pi/3) \leq \theta < 2\pi/3$; $v_{ap}(\theta)=2V_i/3$; $v_{as}'(\theta)= 2V_o'/3$

$$iap=\frac{(2Vi-2Vo')}{3\omega L}(\theta - ø - \pi/3) + iap(ø + \pi/3) \quad (2.5)$$

· Mode 5 : $2\pi/3 \leq \theta < (ø +2\pi/3)$; $v_{ap}(\theta)=V_i/3$; $v_{as}'(\theta)= 2V_o'/3$

$$iap=\frac{(Vi-2Vo')}{3\omega L}(\theta - 2\pi/3) + iap(2\pi/3) \quad (2.6)$$

· Mode 6 : $(ø +2\pi/3) \leq \theta < \pi$; $v_{ap}(\theta)=V_i/3$; $v_{as}'(\theta)= V_o'/3$

$$iap=\frac{(Vi-Vo')}{3\omega L}(\theta - ø - 2\pi/3) + iap(ø + 2\pi/3) \quad (2.7)$$

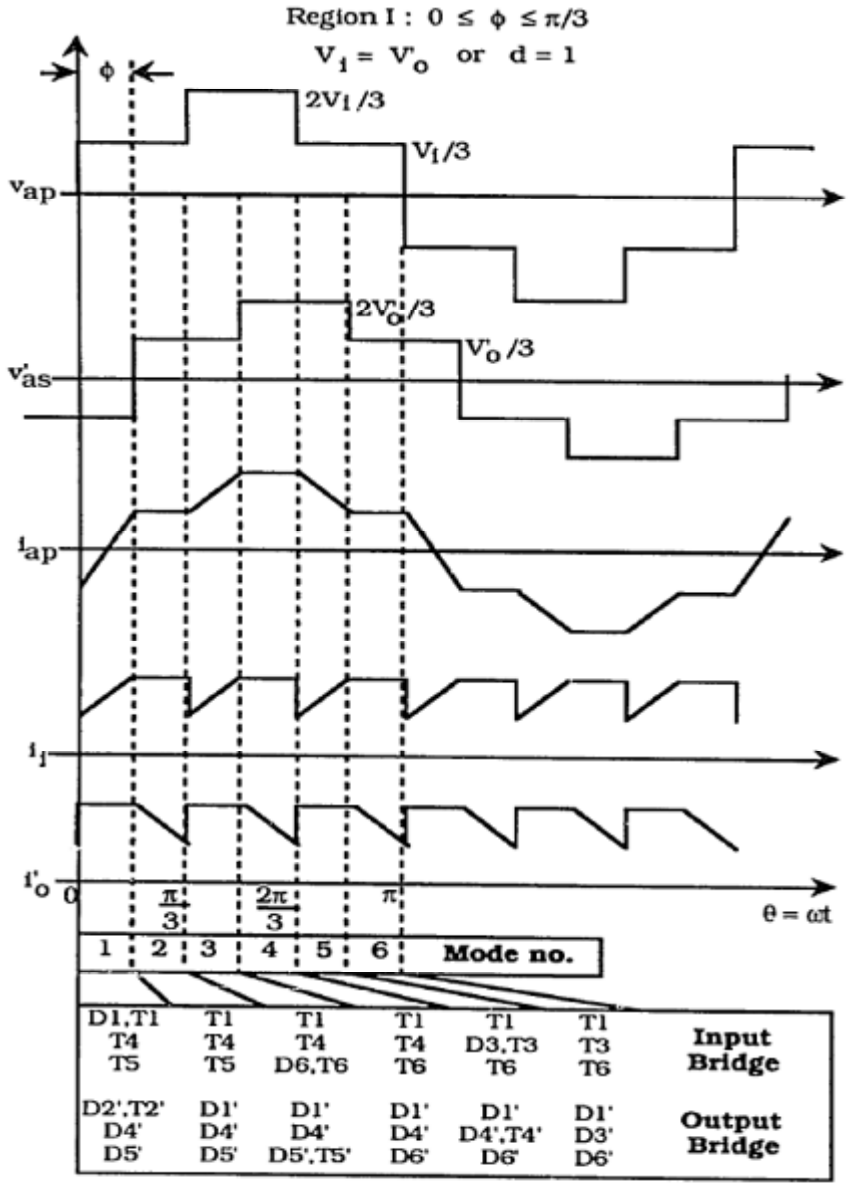

Figure 2.10. The idealized waveforms of phase shift modulation for TPDAB in region I (Kheraluwala et al., 1991)

Region II

· Mode 1 : $0 \leq \theta < (\phi - \pi/3)$; $v_{ap}(\theta)=Vi/3$; $v_{as}'(\theta)= -2V_o'/3$

$$iap(\theta)=\frac{Vi+2Vo'}{3\omega L}(\theta) + iap(0) \quad (2.8)$$

· Mode 2 : $(\phi - \pi/3) \leq \theta < \pi/3$; $v_{ap}(\theta)=V_i/3$; $v_{as}'(\theta)= - V_o'/3$

$$iap=\frac{(Vi+Vo')}{3\omega L}(\theta - \phi + \pi/3) + iap(\phi - \pi/3) \quad (2.9)$$

· Mode 3 : $\pi/3 \leq \theta < \phi$; $v_{ap}(\theta)=2V_i/3$; $v_{as}'(\theta)= -V_o'/3$

$$iap=\frac{(2Vi+Vo')}{3\omega L}(\theta - \pi/3) + iap(\pi/3) \quad (2.10)$$

· Mode 4 : $\phi \leq \theta < 2\pi/3$; $v_{ap}(\theta)=2V_i/3$; $v_{as}'(\theta)= V_o'/3$

$$iap=\frac{(2Vi-Vo')}{3\omega L}(\theta - \phi) + iap(\phi) \quad (2.11)$$

· Mode 5 : $2\pi/3 \leq \theta < (\phi + \pi/3)$; $v_{ap}(\theta)=V_i/3$; $v_{as}'(\theta)= V_o'/3$

$$iap=\frac{(Vi-Vo')}{3\omega L}(\theta - 2\pi/3) + iap(2\pi/3) \quad (2.12)$$

· Mode 6 : $(\phi + \pi/3) \leq \theta < \pi$; $v_{ap}(\theta)=V_i/3$; $v_{as}'(\theta)= 2V_o'/3$

$$iap=\frac{(Vi-2Vo')}{3\omega L}(\theta - \phi - \pi/3) + iap(\phi + \pi/3) \quad (2.13)$$

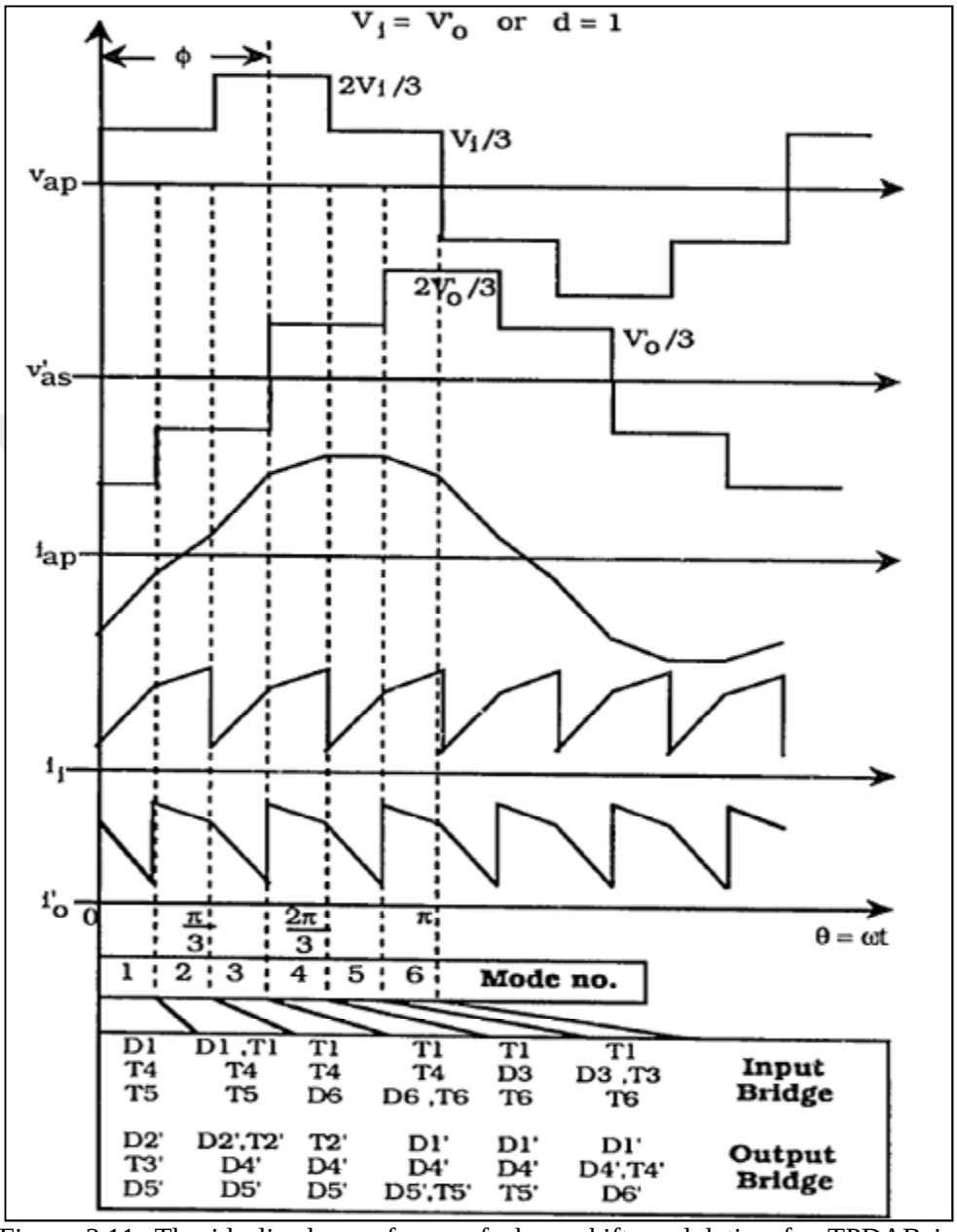

Figure 2.11. The idealized waveforms of phase shift modulation for TPDAB in region II (Kheraluwala et al., 1991)

2.3. Comparison of TPDAB and the SPDAB Converters

Since the TPDAB converters consist of three phase leg, this one extra leg provides reduction in current magnitude comparing to single phase while transferring the same real power (Segaran et al., 2008). Through this extra leg, the switches do not turn-off at maximum current. This feature allows reduction of switching losses (Hoek et al., 2013).

Comparison of Figure 2.7 and Figure 2.11 shows that the inductor current of three phase system is more sinusoidal. This provides reduction of intermediate current harmonics that affect inductor and transformer losses (Segaran et al., 2008). This is another important advantage of the three phase system.

Although the SPDAB converters have some alternative modulation methods, for TPDAB converters the only alternative method is applying 120^{o} phase angle for three phase legs of each of the converter (Segaran et al., 2008).

The TPDAB converters requires more complex control strategy than the SPDAB, however, the single-phase transformer configurations require more magnetic core material, and thereby have more hysteresis losses due to the absence of the flux canceling effect in three-phase transformers. (Baars et al., 2016)

All of these situations can be taken into account while selecting of suitable circuit design strategy

3. DESIGN AND MODELING OF TPDAB CONVERTER

3.1. Introduction

As a result of all the condition discussed in chapter 2, it is important to design a suitable converter according to the application type, the power level requirements, the switching frequency, the filter and the transformer capacity and the size requirements.

An isolated three phase dual active bridge DC-DC converter is designed in this thesis and the railway application operation ranges are considered while determining the design parameters. The design parameters are shown in the Table 3.1. A three phase Y-Y connected isolation transformer is also connected between two bridges with series inductors located in both primary and secondary side of the transformer. Suitable capacitors are used according to voltage and the current requirements.

Table 3.1. The design parameters of TPDAB

Parameter	Value
Input DC Voltage	600 V
Output DC Voltage	800 V
Power	80 kW
Switching Frequency	20 kHz

Measurement and the control systems are designed with suitable sampling times to provide maximum performance and stability. Efficiency analyzes under steady operation and the stability performance under unstable conditions analyzes are also applied for the designed circuit.

3.2. The Power Circuit Design

For the power circuit section, the rating values of the fundamental power circuit components, such as IGBT, transformer, capacitors, are determined. There are some parameters that directly affect the operation of circuit. Therefore the calculations are very important to provide an effective design.

Since the phase shift method is used for the operation of the converter, the first issue is switching frequency and the duty cycle "D". Due to the two control variables, duty cycle D and phase shift angle "ø", the operation will be more complicated for TPDAB converters. Therefore fixed duty cycle is selected for this design circuit and determined as %50 to prevent reactive power circulation. As explained in the section 2.1.2 there are some limitations for determination of the switching frequency based on acceptable harmonic performance, AC fundamental frequency, the transformer and the inductor design. The switching frequency is determined as 20 kHz.

The other important condition is phase shift angle "ø" for TPDAB converters. In (Schibli, 2000), the phase shift angle for maximum power transfer defined as ± π/2. This value is also determined for this design circuit.

3.2.1. Total Equivalent Inductance

After the determination of the switching frequency, the duty cycle, the maximum phase shift angle, the next step is, to determine the total equivalent inductance. The total equivalent inductance consists of transformer leakage inductance and the series inductor. The Eq.3.1. (Kheraluwala et al., 1992) is used for determining the total inductance value when ø is equal to ± π/2. Where Po is 80 kW,Vi is 600 V, d is Vo/Vi, ø is ± π/2, ω is 2πfs and the L is total equivalent inductance of the circuit.

$$Po = \left[\frac{Vi^2}{\omega L}\right].d.[ø - \frac{ø^2}{\pi} - \frac{\pi}{18}] \quad (3.1)$$

As a result of the Eq. 3.1, L is found as 29.16 µH. Since the Eq. 3.1 is valid for under ideal operating conditions and the values that used in the simulation are selected from real datasheet values for each component, providing 100 A maximum output current requires reducing this value to the 20 µH.

3.2.2. The High Frequency Transformer

Another important equipment of the TPDAB converter is the high frequency transformer (HFT). This transformer provides not only isolation, but also efficient system design by adjusting turning ratio. The major differences between primary and secondary DC voltages will cause high RMS and peak currents (Wang, 2012). Therefore, the transformer turn ratio is determined as (1:1.33) based on the parameters in Table 3.1.

Another advantage of using high frequency transformer is, contribution to the size and the cost. The replacement of bulky injection transformers by HFT makes possible to reduce the size weight and also cost of the system (Savrun, 2017). This feature is very important for some applications, such as railway and automotive applications that require minimum size and weight for components. The comparative sizes of the 50 Hz and the 20 kHz transformers are shown in Figure 3.1. Table 3.2 shows the high frequency transformer specification of the circuit.

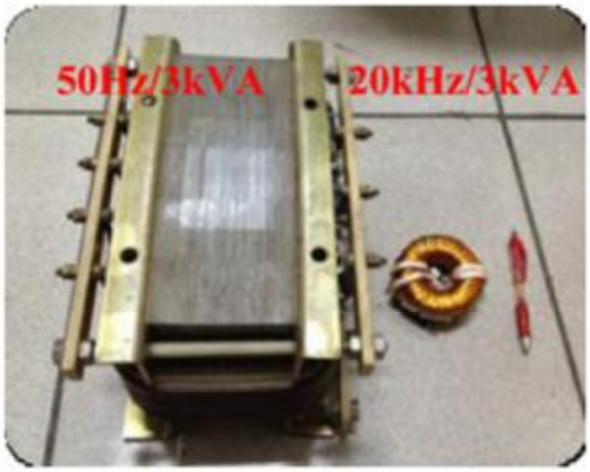

Figure 3.1. The comparative photos of the 50 Hz and the 20 kHz transformers (Zhao et al., 2014)

Table 3.2. The high frequency transformer specifications

Parameter	Value
Primary Voltage	600 V
Secondary Voltage	800 V
Nominal Power	100 kVA
Nominal Frequency	20 kHz
Primary Winding Resistance	0.06 ohm
Secondary Winding Resistance	0.08 ohm
Primary Inductance	6 µH
Secondary Inductance	8 µH

3.2.2. The Switching Device

One of the main components of a dual active bridge circuits, is switching device. It is very important to select suitable switching device that meet the operation frequency and current requirements.

Figure 3.2 shows the comparison of power ratings and switching speed of gate controlled power electronic devices. The result of considering both the converter circuit parameters in the Table 3.1 and the Figure 3.4, demonstrates that the IGBT is the most suitable device for this operating ranges.

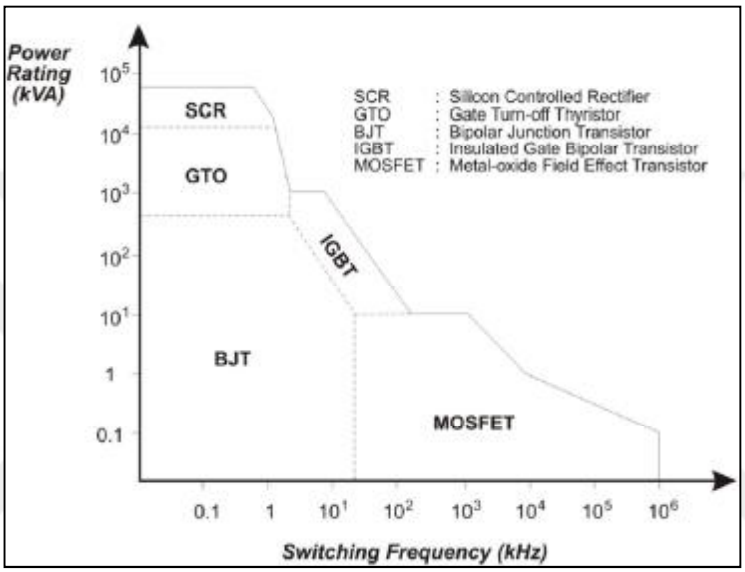

Figure 3.2. Performance limits of gate controlled devices (Barnes, 2003)

In this thesis 1200 V 120 A IGBTs selected as switching device and its parameters are used according to “Semikron Datasheet” that attached in Appendix A.

3.2.3. DC Link Filter Capacitors

Although the TPDAB converter requires less capacitor filter size because of the advantage of being multiphase, there are still some requirements of filter capacitors based on the maximum load current, switching frequency and the output DC voltage. In (Schibli, 2000) the minimum required output DC link filter capacitor is calculated using Eq.3.3 (Kheraluwala et al., 1992). .

$$Co = 50.\left[\frac{io}{Vo.fsw}\right] \quad (3.3)$$

Since the maximum output power is 80 kW and the output DC voltage is 800 V the maximum load current i_o is 100 A and switching frequency is 20 kHz and as defined before. After this calculation the minimum required output filter capacitor is found 312.5 µF. Based on current and voltage requirements, following capacitor is selected and connected as parallel to meet the current requirements. The capacitor datasheet attached in the Appendix B.

$V_{R\,DC}$ = 900 V DC / V_{TT} = 1350V DC, 10 s / V_{TC} = 4000 V AC, 10 s

C_R µF	I_{MAX} [1] A	I_s kA	$\hat{I}$ kA	ESR [2] mΩ	L_{self} nH	R_{TH} K/W	D mm	H_C mm	H_T mm	Weight kg	Fig.	Ordering code
220	50	10.8	3.6	1.3	≤ 40	4.0	85	70	76	0.45	1	B25620B0227K881
220	50	10.8	3.6	1.3	≤ 40	4.0	85	74	76	0.48	2	B25620C0227K881
350	50	10.7	3.6	1.5	≤ 40	3.3	85	95	101	0.58	1	B25620B0357K881
350	50	10.7	3.6	1.5	≤ 40	3.3	85	99	101	0.61	2	B25620C0357K881
420	60	11.9	4.0	1.4	≤ 40	3.0	90	95	124	0.73	3	B25623B0427K904
440	65	21.7	7.2	0.8	≤ 40	2.9	116	70	76	0.88	4	B25620B0447K883
480	55	10.8	3.6	2.0	≤ 40	2.9	85	120	126	0.71	1	B25620B0487K881
480	55	10.8	3.6	2.0	≤ 40	2.9	85	124	126	0.74	2	B25620C0487K881
550	50	11	3.7	2.8	≤ 40	2.8	85	132	138	0.87	1	B25620B0557K881
550	50	11	3.7	2.8	≤ 40	2.8	85	136	138	0.9	2	B25620C0557K881
580	62	11.9	4.0	1.8	≤ 40	2.8	90	120	149	0.9	3	B25623B0587K904
650	62	11.8	3.9	2.0	≤ 40	2.5	90	132	161	1	3	B25623B0657K904
700	70	21.5	7.1	1.3	≤ 40	2.3	116	95	101	1.13	4	B25620B0707K883
730	62	11.8	3.9	2.8	≤ 60	2.3	90	145	174	1.2	3	B25623B0737K904
750	75	23.1	7.7	1.1	≤ 60	2.1	85	173	179	1.1	1	B25620B0757K881
750	75	23.1	7.7	1.1	≤ 60	2.1	85	177	179	1.13	2	B25620C0757K881
830	75	23.5	7.8	1.5	≤ 60	2.0	90	173	202	1.3	3	B25623B0837K904
970	75	21.7	7.2	1.9	≤ 40	2.2	116	120	126	1.4	4	B25620B0977K883
1100	80	21.7	7.2	1.4	≤ 40	2.1	116	132	138	1.55	4	B25620B0118K883
1500	100	43	15.4	1.1	≤ 60	2.0	116	173	179	1.945	4	B25620B0158K883
1500	100	43	15.4	1.1	≤ 60	2.0	116	177	179	1.945	5	B25620C0158K883

Figure 3.3. The DC link filter capacitor datasheet values

3.3. Controller Design

After designing the power circuit model, another important issue is to control all switching components and the system operation. Gate signal generator, control of power transmission, response of the changes in system and the measurements are all part of this controller system.

The basic structure of the DAB controller is shown in Figure 3.4. As shown it starts with the feedback control, that compares the set and the actual values. The difference between the $V_{o,set}$ and $V_{o,actual}$ quantities, produces the V_{err} signal which is also an input of the PI controller. The PI controller determines the applied phase shift angle and the power flow direction and this process continues with the "limiter" section that keeps the phase shift angle in a particular interval.

After limitations the produced output signal is implemented to the IGBT gates via "Gate Signal Generator".

The implementation of these structures in MATLAB requires creation of separate blocks. The blocks are created as MATLAB functions and separate sample times are selected for them based on the sensitivity of process.

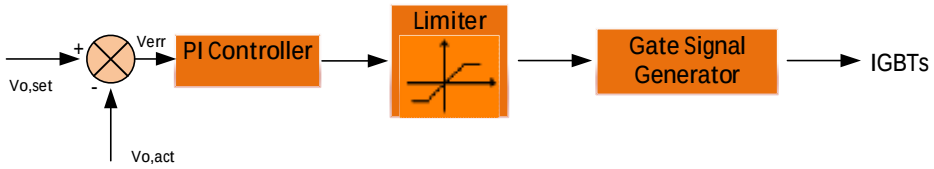

Figure 3.4. The control structure of DAB DC-DC converter

3.3.1. PI Controller

The implementation of phase shift angle and the determination of the power flow direction are provided by a PI controller. As shown in the Figure 3.5 in PI controller, the set and the actual values is compared and some additional processes is applied to the difference of these two quantities and the output signal

is produced. The output signal comprises the amplified difference and the integral of the difference between the set and the actual values (Cheung, 2017).

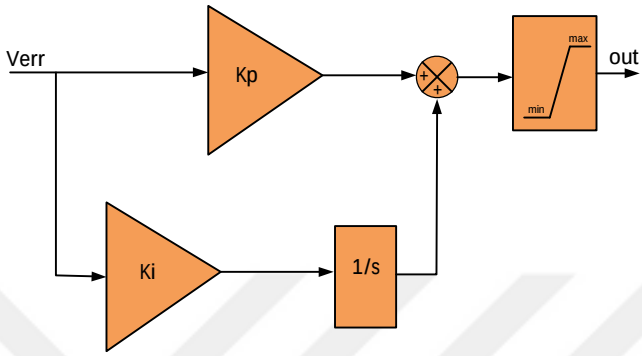

Figure 3.5. PI controller block diagram

The implementation of this PI controller block scheme in the MATLAB function, requires summation of set and the actual value in a sample time interval which generally absorbed into the “Ki” term.

As shown in the Figure 3.6 the PI controller in MATLAB consists of two inputs and one output, that are also an input of the “IGBT Gate Signal Generator Function”. The sampling time interval is identified as 50 µs for this function block.

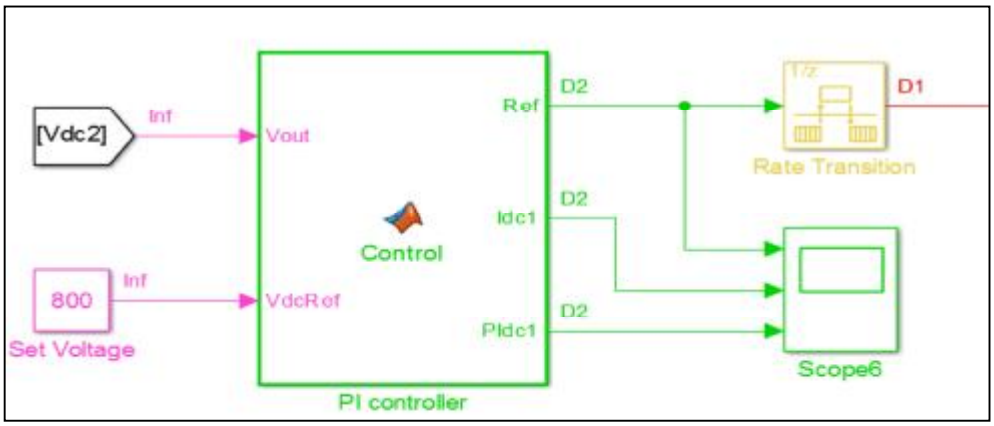

Figure 3.6. The PI controller block in MATLAB/Simulink

As shown in the Figure 3.7 , the error signal which is the summation of set and the actual values, amplified with Kp constant. This result is added to the integral of error signal by amplifying with Ki constant and the sampling time. As described in the previous chapters the phase shift angle for maximum power transfer defined as ± π/2 (Schibli, 2000). This issue is considered in the PI controller block and the output signal is limited as ± 90 as shown in the Figure 3.7. All function block codes of the controller circuit, are attached in the Appendix C.

The output signal is connected to the “Gate Signal Generator” block as input. Since both of these blocks have different sample times, the connection of these blocks requires additional block called “Rate Transition”.

```
function [Ref,Idc1, PIdc1]  = Control(Vout, VdcRef)
%#codegen
global VdcErr;
global Pdc;
global Idc;
global PIdc;

Kp=3;
Ki=50;

Ts=50e-6;

LimPIp=90;
LimPIn=-90;

VdcErr = VdcRef - Vout;
Pdc = Kp*VdcErr;
Idc = Idc + Ki*Ts*VdcErr;
PIdc = Pdc + Idc;
if PIdc > LimPIp
    PIdc = LimPIp;
    Idc = LimPIp;
end
if PIdc < LimPIn
    PIdc = LimPIn;
    Idc = LimPIn;
end

Ref = (PIdc/360);
Idc1=Idc;
PIdc1=PIdc;



end
```

Figure 3.7. The PI controller function block codes

3.3.2. Gate Signal Generator

Each side of the TPDAB converters consists of 6 IGBTs and the general switching sequence of three phase inverters is shown in the Figure 3.8 based on 180^{o} conduction mode.

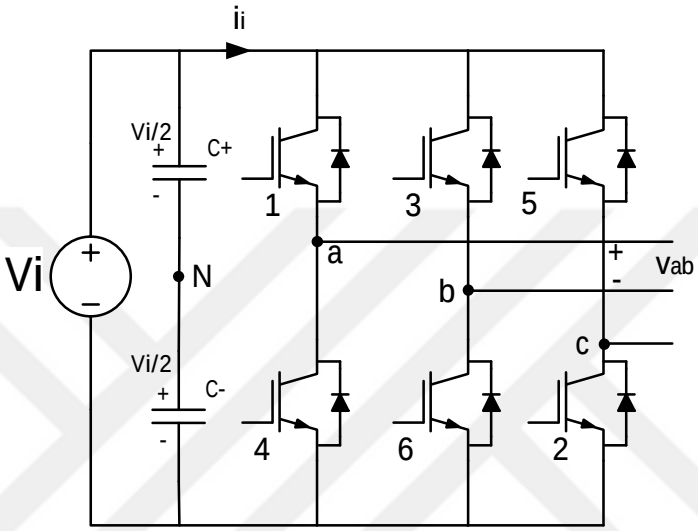

(a)

On	Off	STATE	v_{ab}	v_{bc}	v_{ac}
T1,T2,T6	T4,T5,T3	1	v_i	0	$-v_i$
T2,T3,T1	T5,T6,T4	2	0	v_i	$-v_i$
T3,T4,T2	T6,T1,T5	3	$-v_i$	v_i	0
T4,T5,T3	T1,T2,T6	4	$-v_i$	0	v_i
T5,T6,T4	T2,T3,T1	5	0	$-v_i$	v_i
T6,T1,T5	T3,T4,T2	6	v_i	$-v_i$	0
T1,T3,T5	T4,T6,T2	7	0	0	0
T4,T6,T2	T1,T3,T5	8	0	0	0

(b)

Figure 3.8. Three phase inverter circuit (a) and switching sequence (b)

In the “Gate Signal Generator” block, the switching states for each side of IGBTs and the phase shift conditions are implemented. Figure 3.9 shows the gate signal generator block in Simulink. The sample time of this block is determined as 0.5 µs to achieve sensitive operation. The PI controller output “Ref” signal, and a 20 kHz saw-tooth signal (with peak of -1 to +1), are used to implement the phase shift angle. The MATLAB function block codes of the gate signal generator block is attached in the Appendix C. As a result of this function block, the produced gate signal of the first side converter is shown in the Figure 3.9. The upper IGBT gate signals of the first side and the second side converters after applied phase shift, are shown in the Figure 3.14.

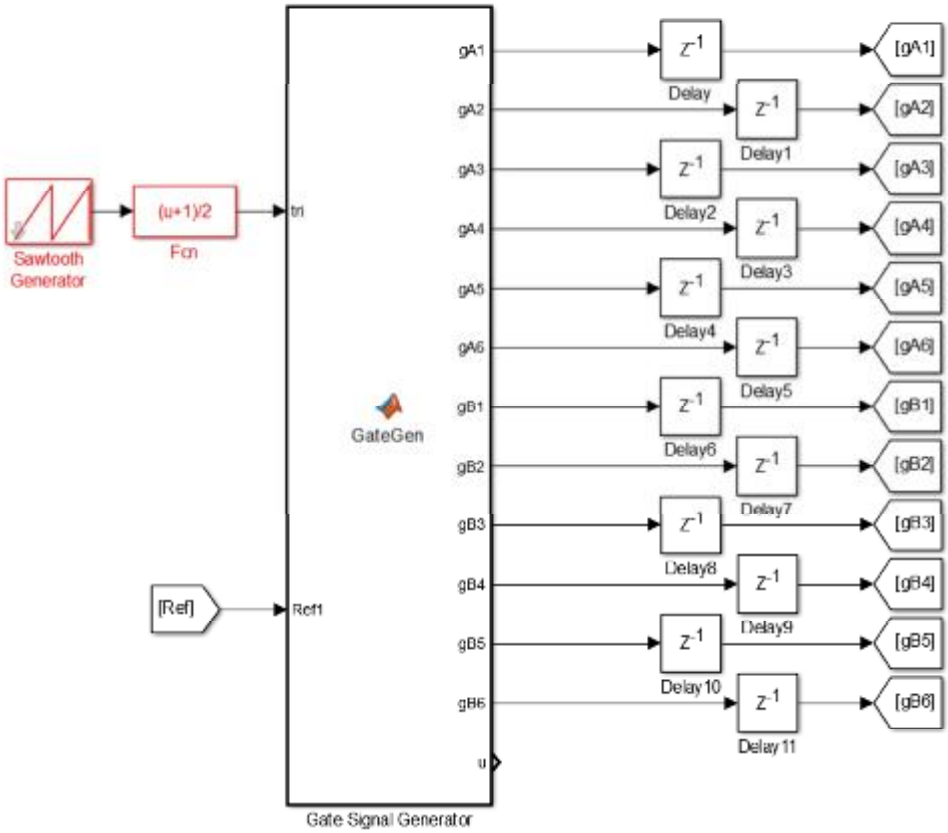

Figure 3.9. Gate signal generator block in Simulink

3.3.3. Control of Power Flow

In previous sections, all parts of the simulation model were described separately. In this chapter the integration of all these parts will be discussed to explain overall system operation. As shown in the Figure 3.23 the simulation consists of power circuit, PI controller, gate signal generator and the measurement systems.

In PI controller the set and the actual values of output DC voltage is compared. The value of the output signal “Ref” is defined according to the quantity of this error signal which is the result of summation process of these two voltage values. This “Ref” quantity is also transferred to the gate driver as input by the rate transition block. This “Ref” value is used in gate signal generator block to decide if the phase shift required. The direction of phase shift is also defined by this value. According to the change of the output voltage, this procedure is repeated in every 50 μs.

After implementation of gate signal and the phase shift modulation, the other issue is, controlling the power flow direction and the keeping the output voltage stable even some changes occur in the system. When the output voltage reaches the set voltage, the phase shift process is terminated or when the output voltage exceeds the set voltage, then the phase shift procedure works in negative direction. For instance, if the converter is used in battery charging system, system must be cut power flow when the batteries are fully charged or if the converter used in the railway applications, voltage ripples at the input side or regenerative affect at the output side could occur. These situations must be realized with the measurement systems and handled with the control system to keep the system stable of the converter.

4. SIMULATION RESULTS

4.1. Introduction

After all design calculations and the considerations, the system operation must be verified by a suitable simulation program. Obtaining the realistic simulations results requires adjusting the component parameters as much as close to the reality. The simulation circuit is shown in Figure 4.1. As mentioned in the previous chapters, in applications, especially HEV and railway applications, there can be some unstable situations during operation. For instance, changing of input voltage or fluctuations, changing of load or fluctuations are always possible during the operation.

In this chapter some cases were examined and the results were interpreted. MATLAB/Simulink program are used for the simulations

4.2. Case 1

The normal operation of the circuit is analyzed in this case. The output voltage is set as 800 V and the simulation is started.

In this case the simulation is started as normal start-up. Since the output DC voltage V_o is “0” in the first start-up, PI controller sends the maximum phase shift command to the gate signal generator and the maximum phase shift angle “90^o” is applied to the secondary side gates. When the output DC voltage V_o reaches the set voltage, then the phase shift angle is reduced the value that keep the output voltage stable according to load requirements.

V_o reaches to 800 V at t=0.021. An overshoot, which has 813 V peak voltage between t=0.021 and t=0.18 time intervals depends on PI controller parameters. After t=0.18 V_o is kept around 800 V as shown in Figure 4.2. This figure also shows the relation between phase shift angle and the output DC voltage.

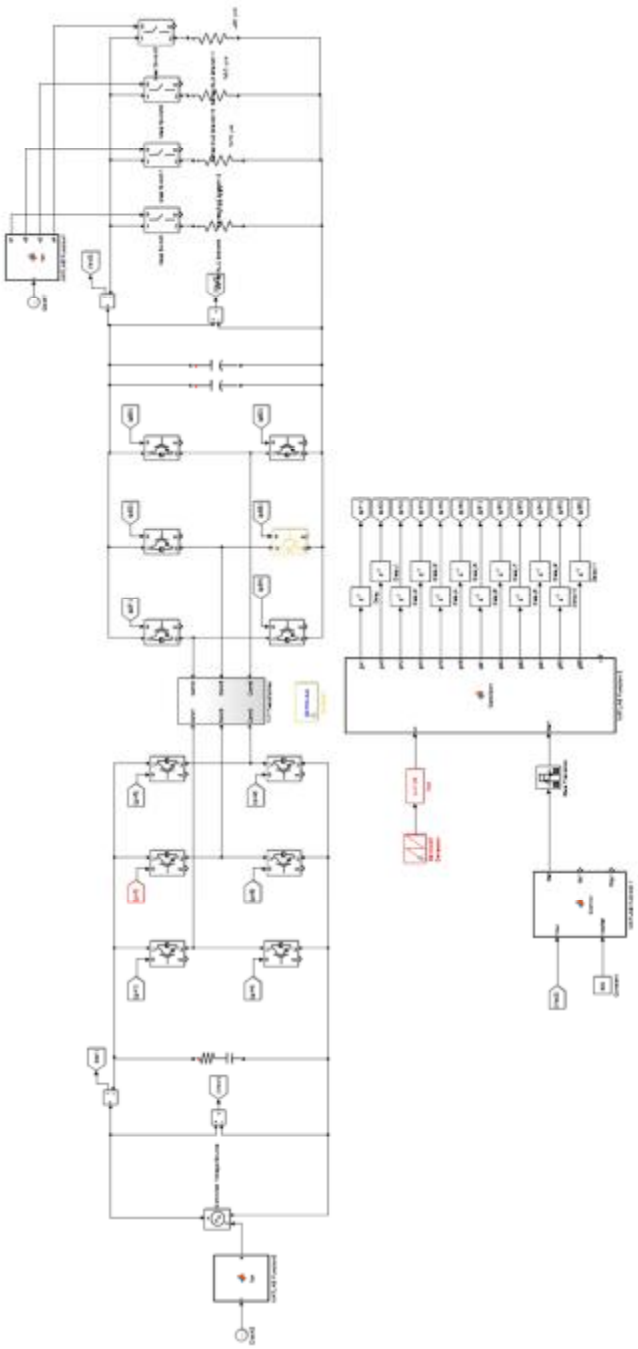

Figure 4.1. The simulation circuit

As shown in the figure the phase angle decreases while the actual set voltage V_o is reaching the set voltage.

Figure 4.3 shows the primary and the secondary AC voltages while the phase shift is applying before the output DC voltage reaches to the set value. Figure 4.4 also shows the waveforms while the phase shift is applying after the output DC voltage reaches to the set value.

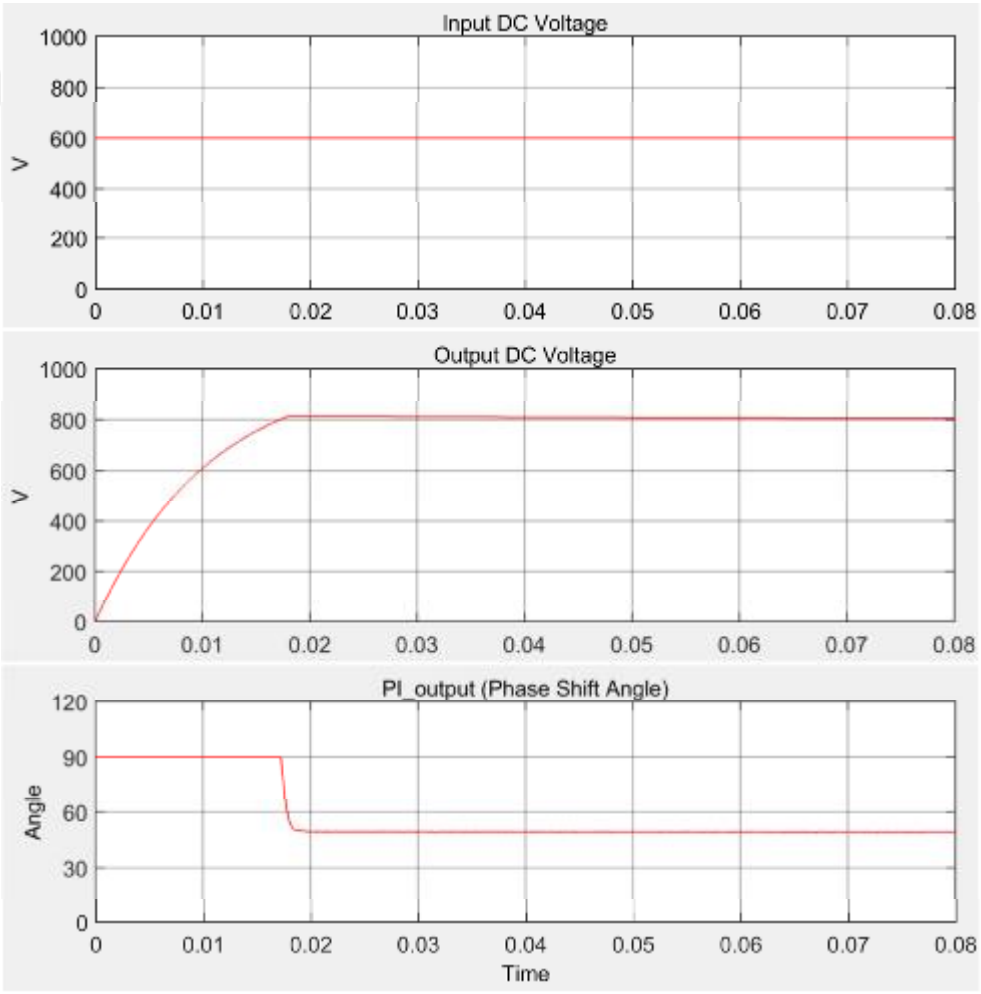

Figure 4.2. The startup input DC voltage, output DC voltage and phase shift angle waveforms

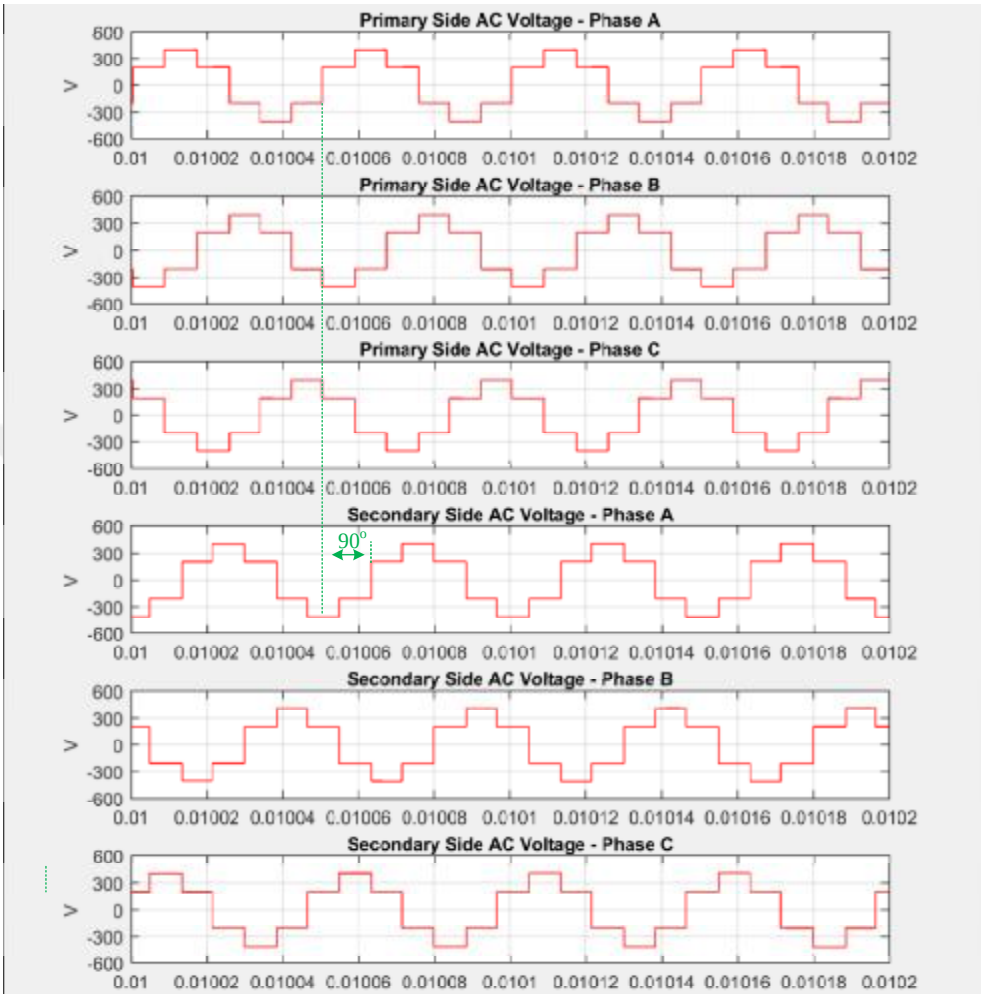

Figure 4.3. The AC voltages of primary and secondary side of the transformer before reaching to set output DC voltage

Figure 4.5 and Figure 4.6 shows the primary and the secondary side of currents for each phase before and after the reach to the output set voltage. The waveforms are similar as compared with the theoretical waveforms in Figure 2.10.

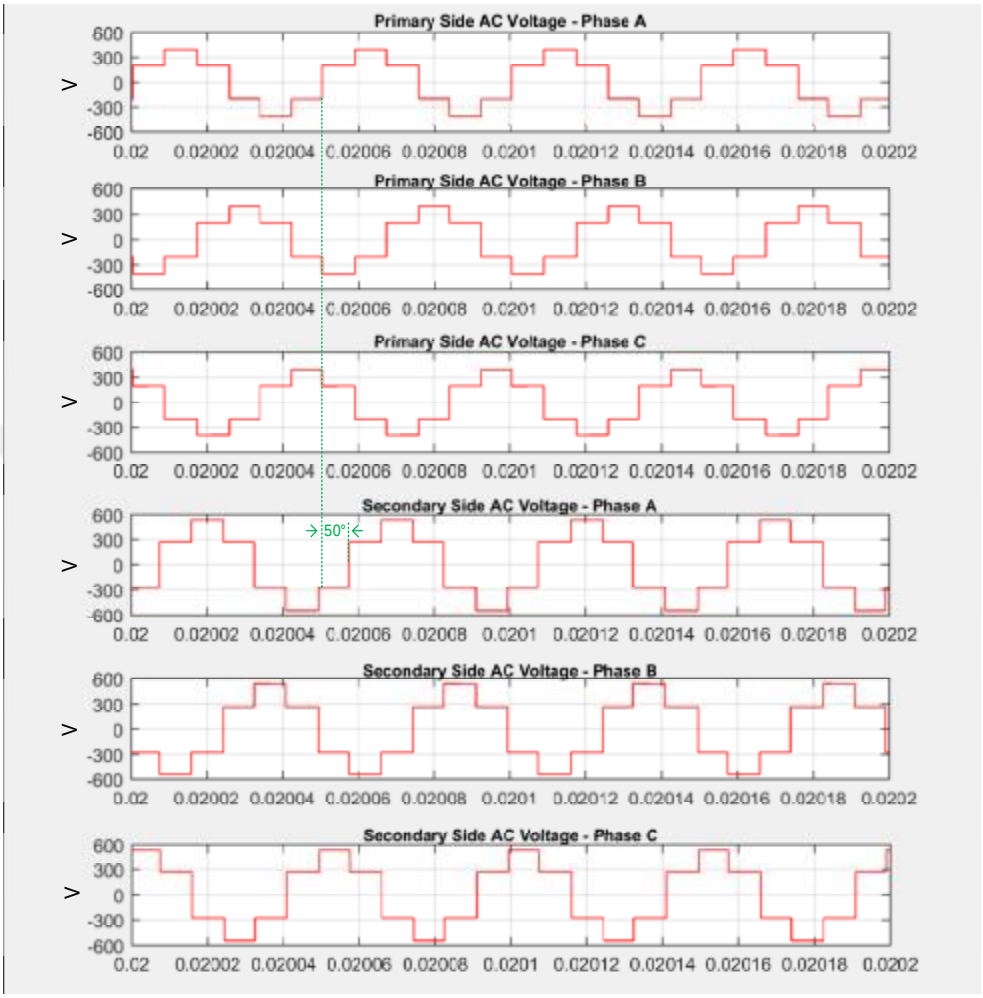

Figure 4.4. The AC voltages of primary and secondary side of the transformer after reaching to set output DC voltage

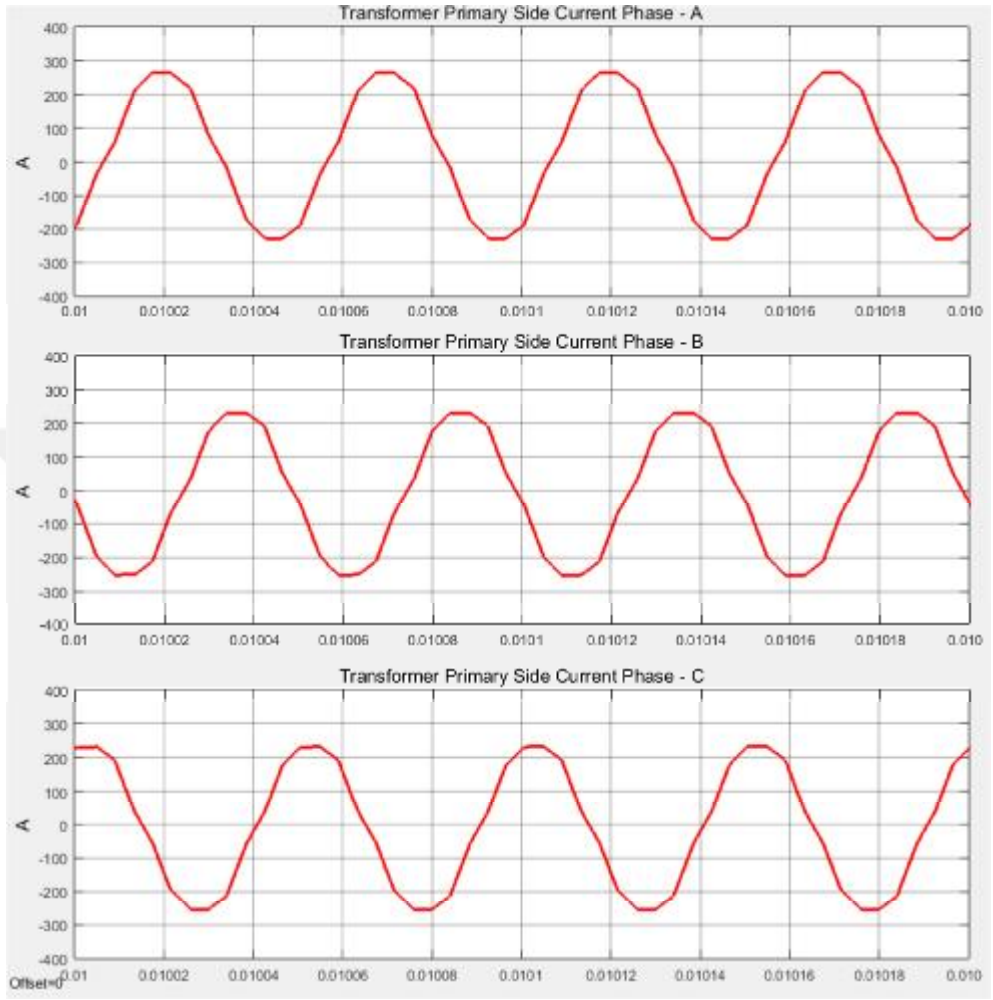

Figure 4.5. The AC currents of primary side of the transformer before reaching to the set output DC voltage

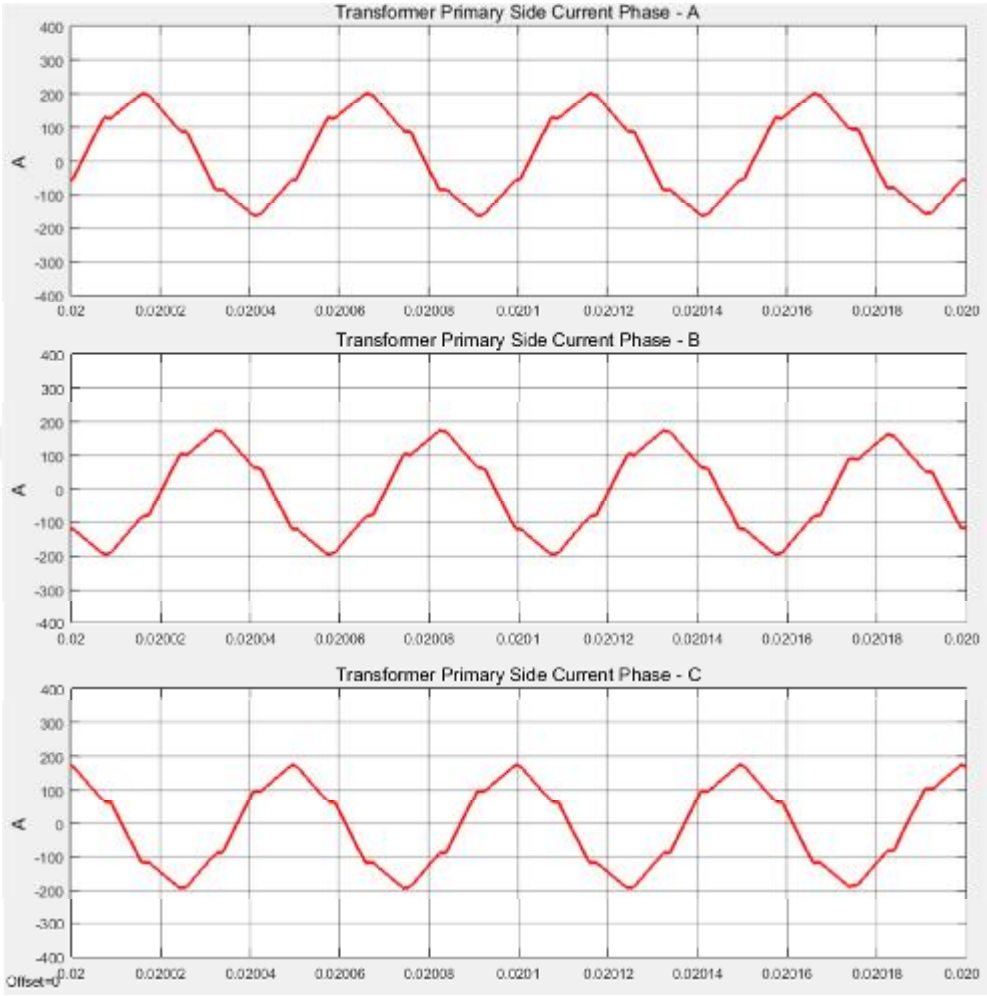

Figure 4.6. The AC currents of primary side of the transformer after reaching to the set output DC voltage

4.3. Case 2

In the case 1, the ideal operating start-up condition was analyzed in one direction. In some high power applications the output voltage V_o can increase depending on regenerative operation of motors. Since the circuit designed as bi-directional DC-DC converter, it is expected to operate in opposite direction of the normal operation.

As shown in the Figure 4.7 while the output DC voltage V_o was around 800 V at t=0.2 suddenly it increases to the value of 900 V. The PI controller applies negative output to provide negative phase shift to the gates. This process continues until the V_o value returns back to the 800 V. Figure 4.8 also shows the AC waveforms of the transformer

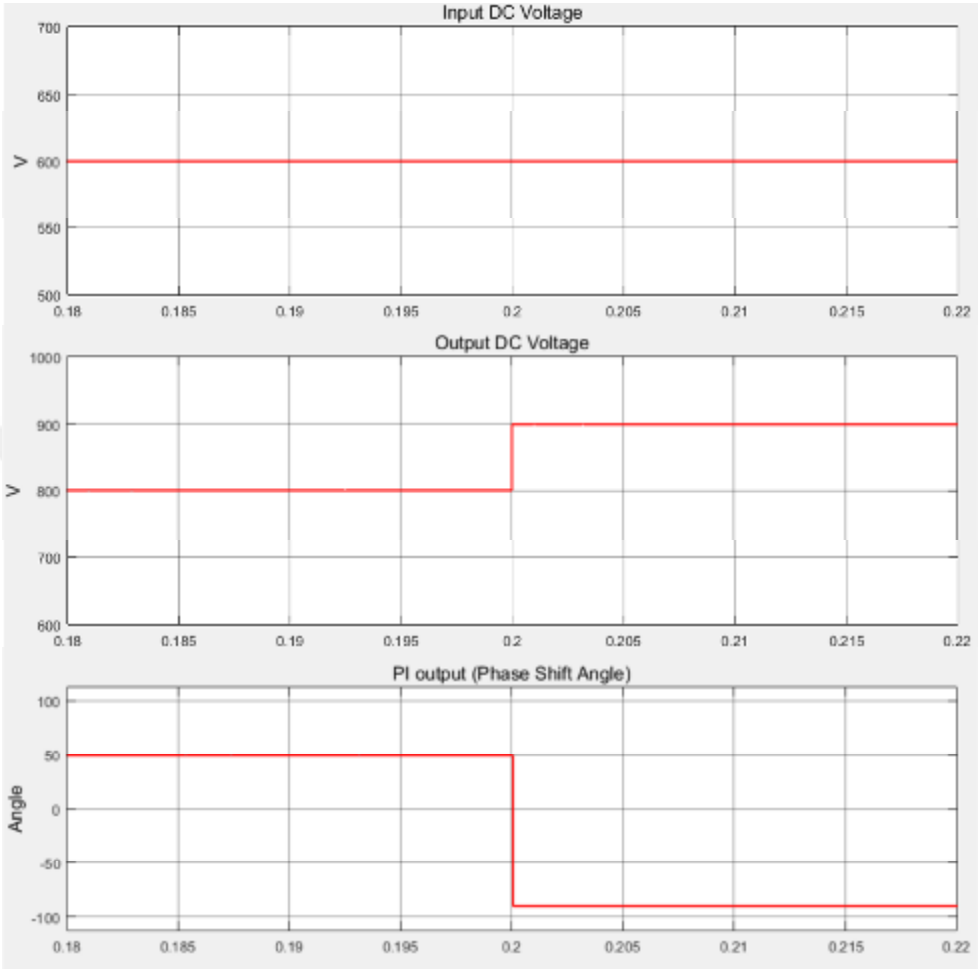

Figure 4.7. The system response to increasing output DC voltage

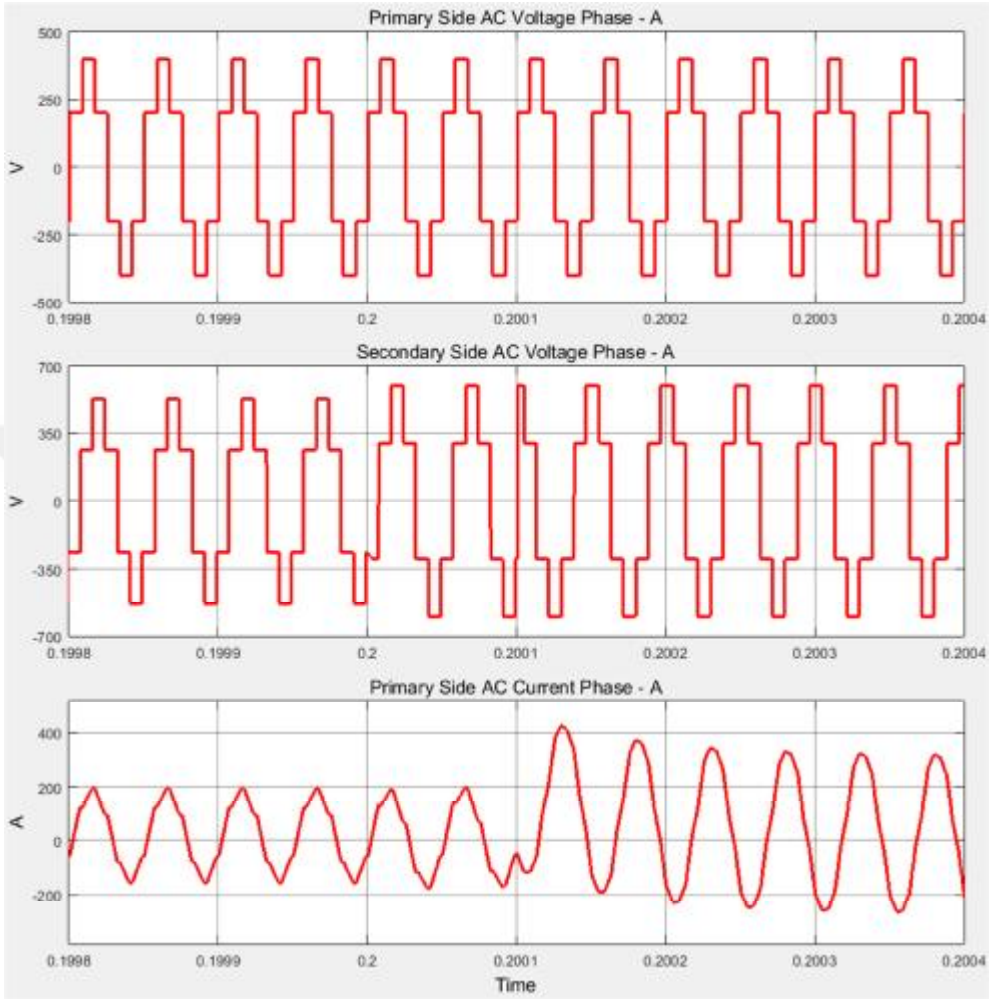

Figure 4.8. The waveforms of increasing output DC voltage

4.4. Case 3

This circuit is supplied from grid and some changes of the input voltage is always possible. The system must handle this situation and keep the output voltage stable. In this case these situations and the system responses are analyzed.

Firstly the increase of input DC voltage V_i is analyzed. Simulation is started normally and at the time t=0.1 second the input DC voltage increased to the value of 660 V. Since the system is designed according to 600 V input voltage, keeping the output DC voltage stable requires decreasing the applied phase shift angle.

As shown in the Figure 4.9 the applied phase shift angle is about 50^o since the output voltage is stable around 800 V depends on load requirements. At time t= 0.1 second when the input voltage V_i is increased, the applied phase shift angle is decreased to a suitable value that keep the V_i is stable. This process continues until the V_i returns to its old value. During all this process V_o is kept around 800 V successfully. Figure 4.10 shows the waveforms of this process.

The other condition is decrease of the input voltage. Similarly the decrease of the input voltage is unwanted condition and keeping stable of output DC voltage requires some increases of applied phase shift angle as shown in the Figure 4.11. As shown in the figure the applied phase shift angle is around 48^o while the input voltage is 600 V and the output voltage is around 800 V. At the time t=0.1 second the input voltage is decreased to the value of 540 V and the applied phase shift angle is increased to the value of 57^o. During all this process V_o is kept around 800 V successfully as shown in the Figure 4.11. The waveforms of this process are also shown in Figure 4.12.

The other analyzed condition is the oscillation of the input voltage for a while. As well as sudden increases and decreases, the oscillation of input voltage is also possible for such a system. As shown in the Figure 4.13, while the input voltage is stable at 600 V while time between t=0.1 and the oscillation of input voltage is applied to the system. The input voltage oscillates between 660 V and

540 V with frequency of 10 kHz. During this time interval, the applied phase shift angle also oscillates keep the output voltage stable around 800 V. This process is also successful as shown in Figure 4.13.The waveforms of the transformer voltages and the currents also shown in Figure 4.14.

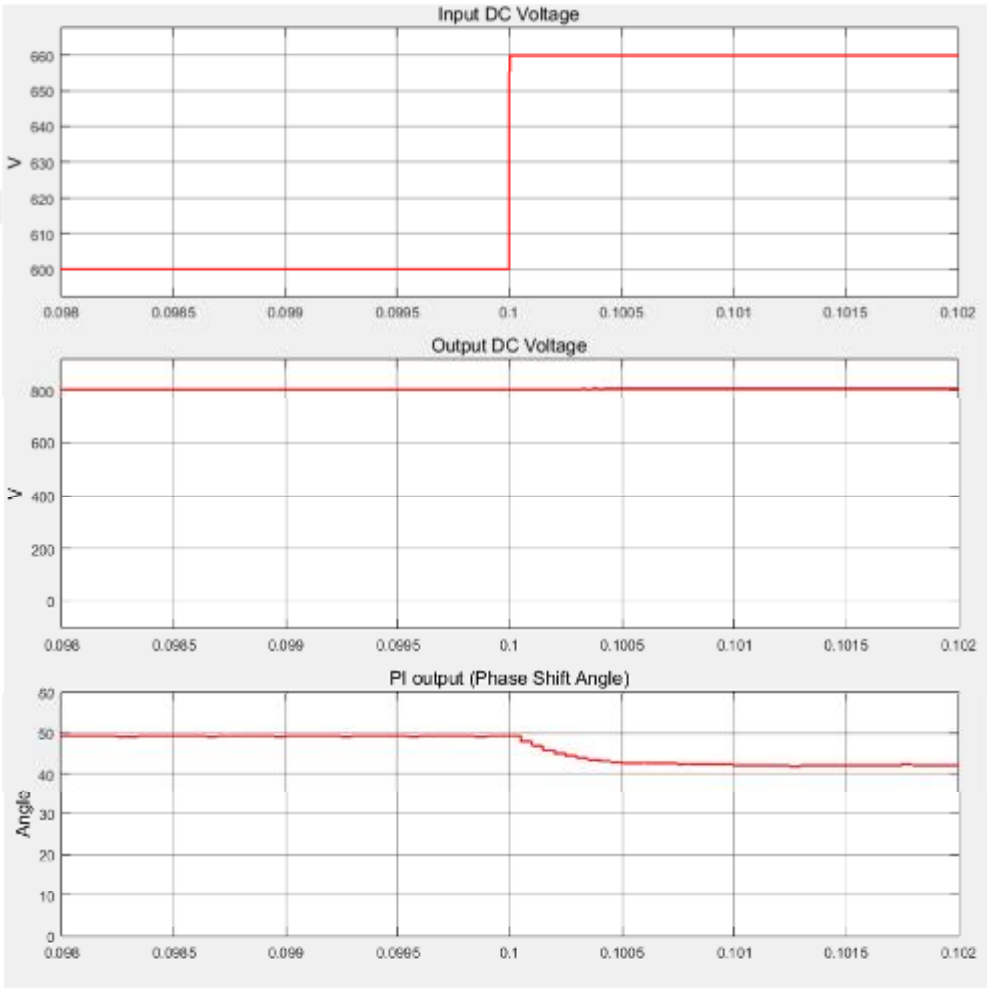

Figure 4.9. The system response to increasing input DC voltage

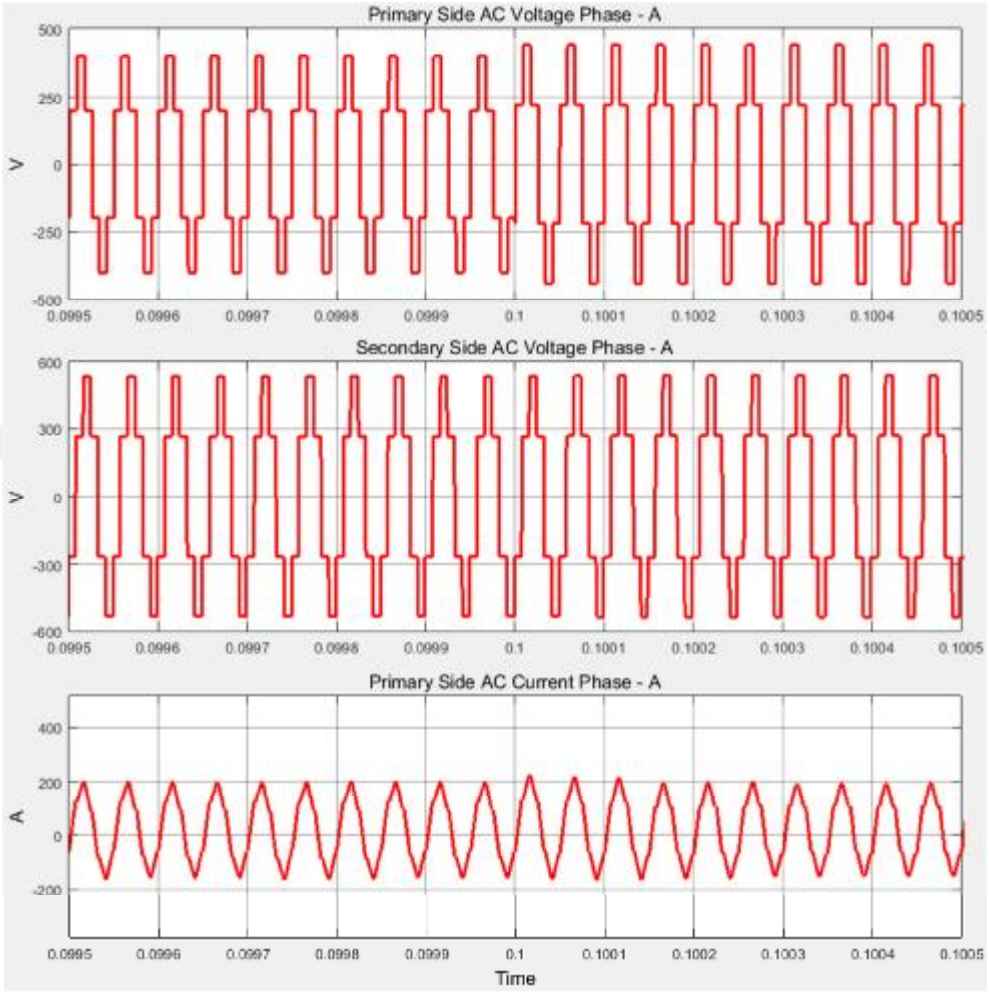

Figure 4.10. The waveforms of increasing input DC voltage

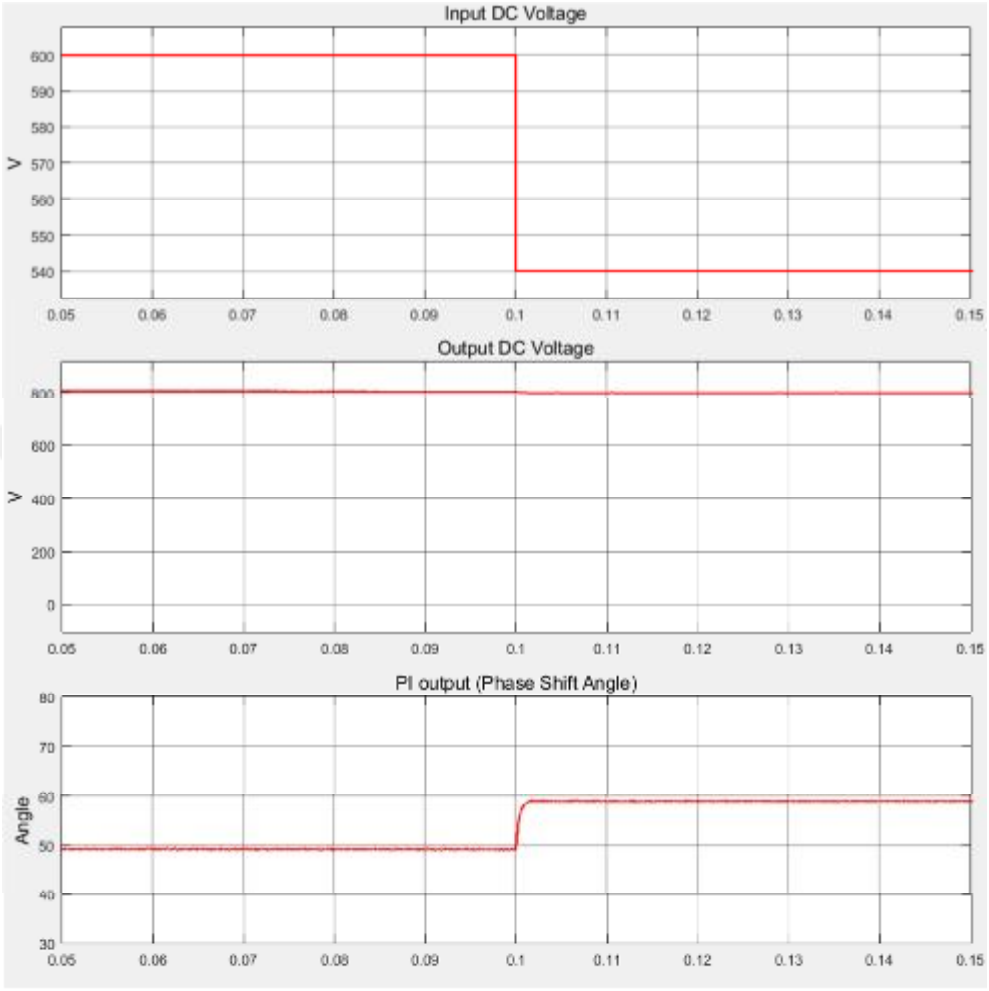

Figure 4.11. The system response to decreasing input DC voltage

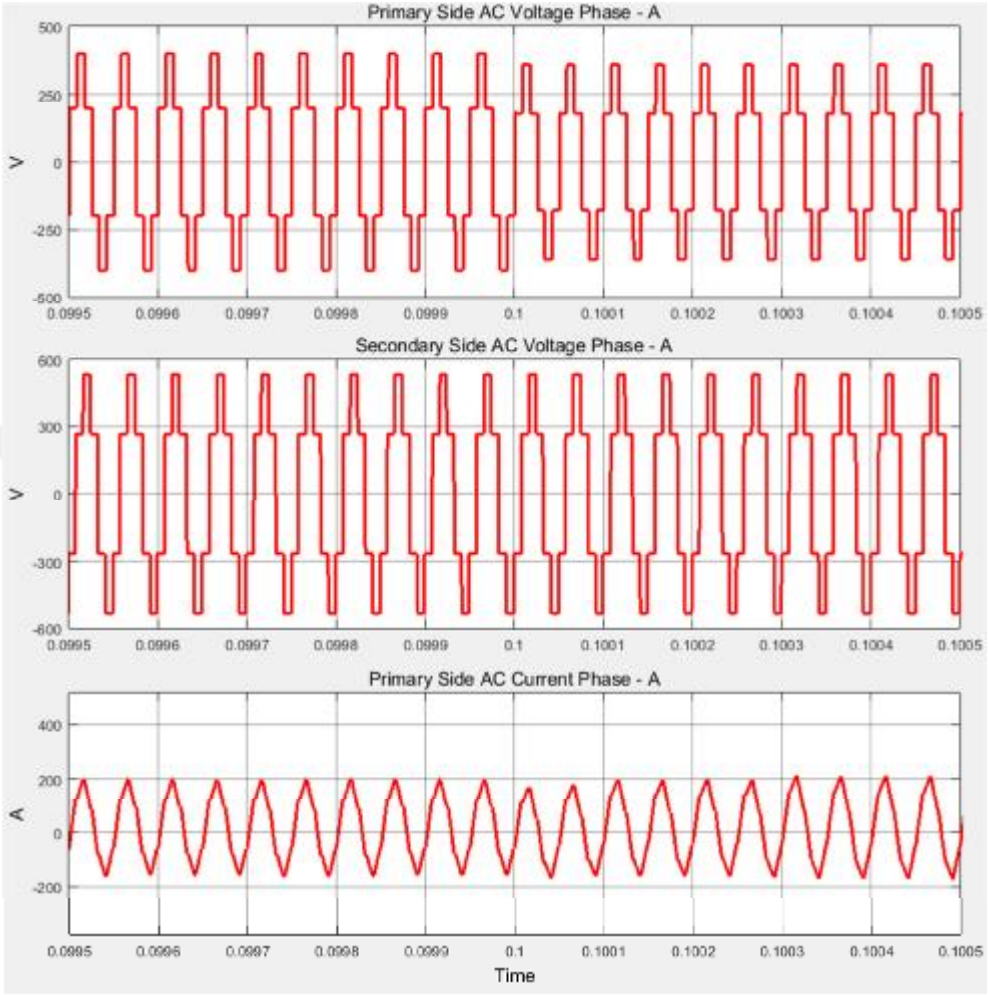

Figure 4.12. The waveforms of decreasing input DC voltage

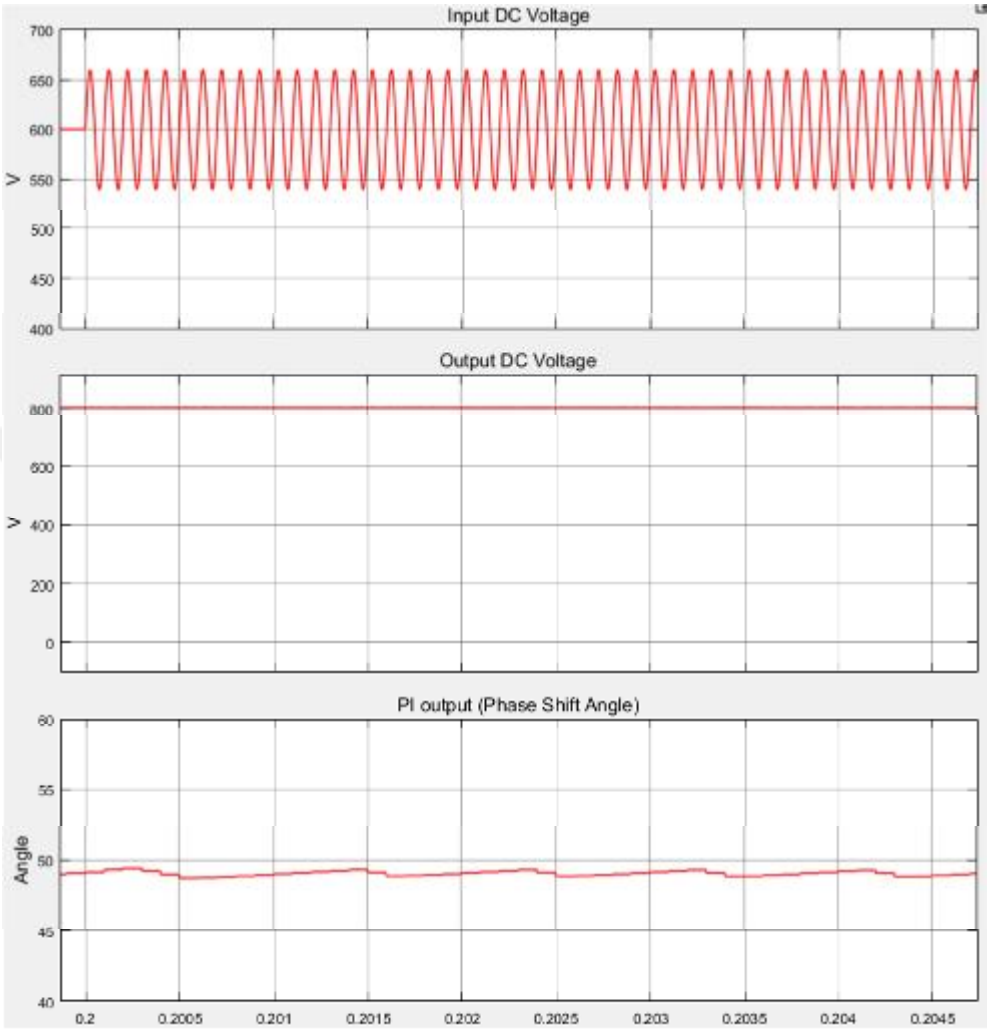

Figure 4.13. The system response to oscillating input DC voltage

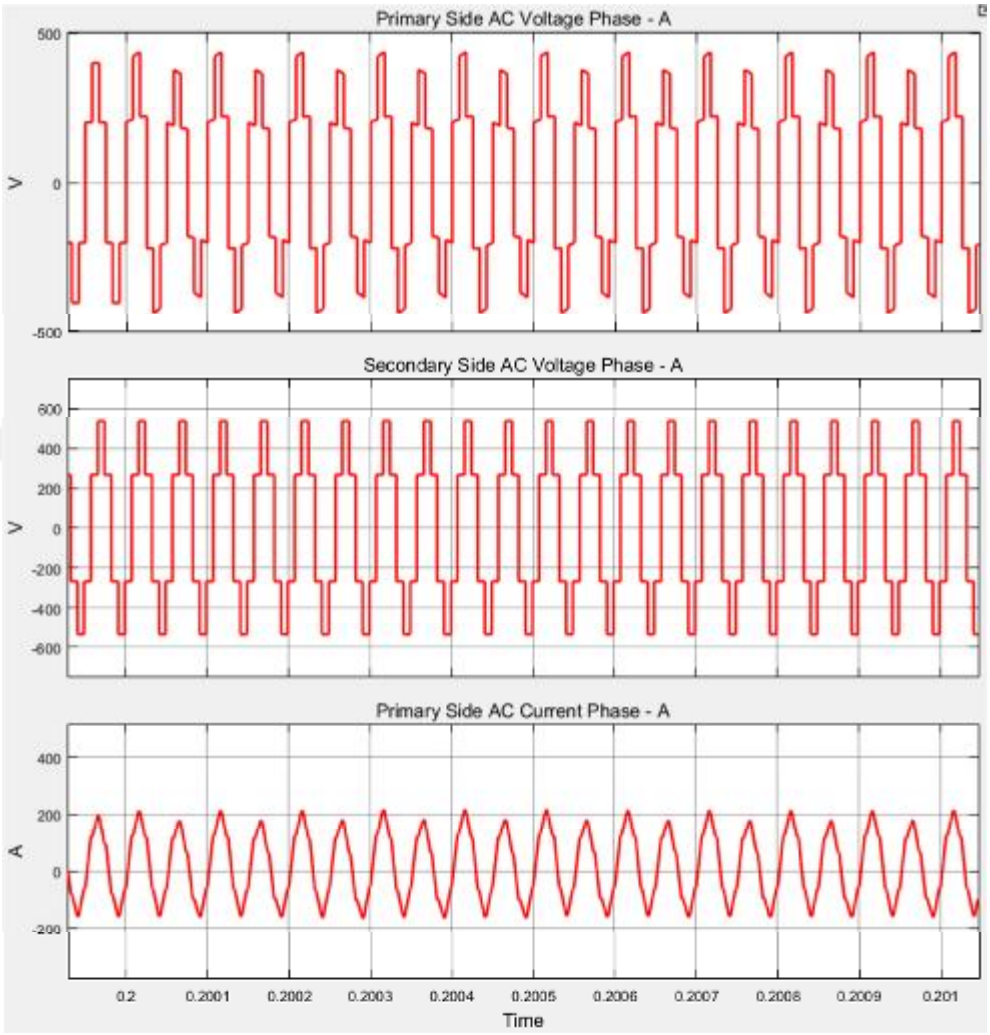

Figure 4.14. The waveforms of oscillating input DC voltage

4.5. Case 4

It is also possible to have some the load conditions changes depends on the application type. When this situation occurs, system must handle this problem and provide the stable output voltage. In this case, the load changes are applied to the system and the system response is analyzed.

System is started with full load operation. At the time t=0.2 the load is decreased suddenly to %75 of full load condition. This process takes 0.2 seconds.

At t=0.4 second, the load is decreased suddenly to %50 of full load condition. This process takes 0.2 seconds. At t=0.6 second, the load is decreased suddenly to %25 of full load condition. This process takes 0.2 seconds. At t=0.8 second, the load is decreased suddenly to %25 of full load condition. This process takes 0.2 seconds. At t=0.8 the load is decreased suddenly to “0” and no load condition is also observed.

V_o tends to be change while some load changes applied to the system. This situation prevents by adjusting of phase shift angle as shown in the Figure 4.15 and the system handles that load changes and achieve to keep the output voltage around 800 V successfully. The AC waveforms are also shown in Figure 4.16

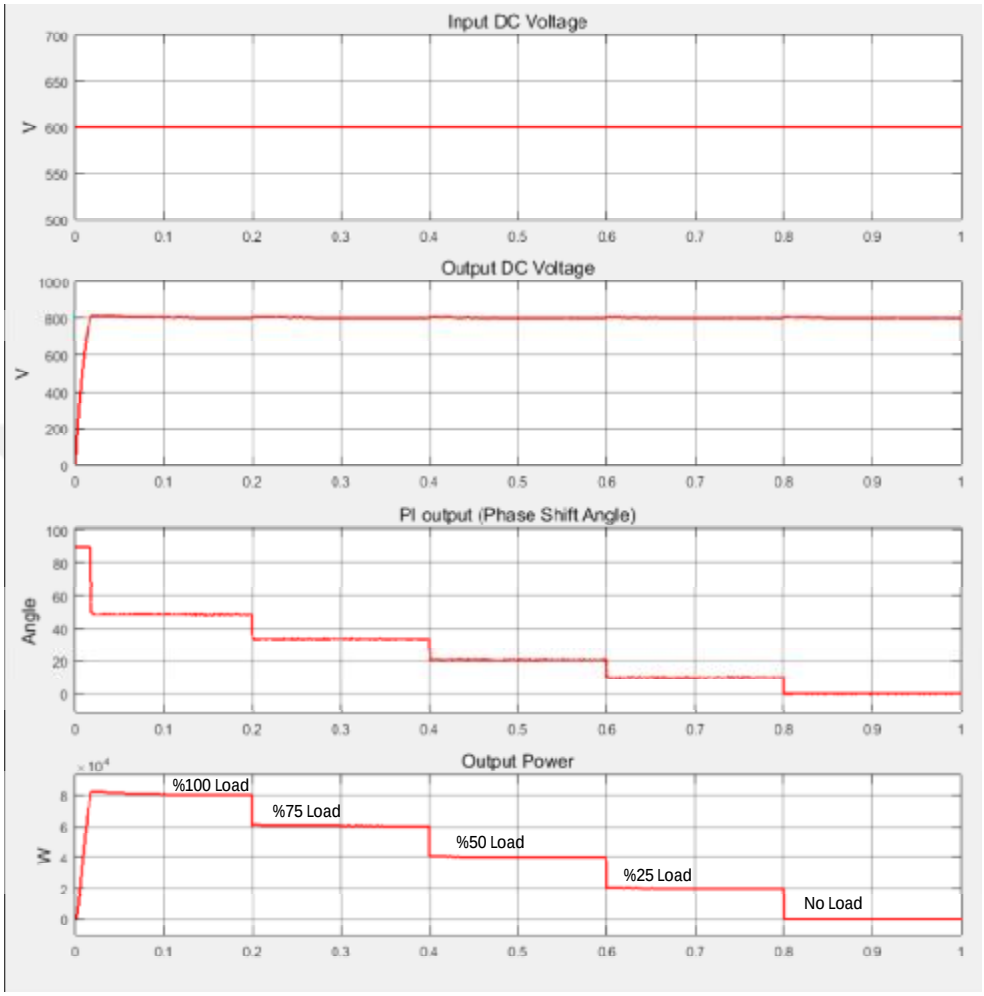

Figure 4.15. The system response to load changes

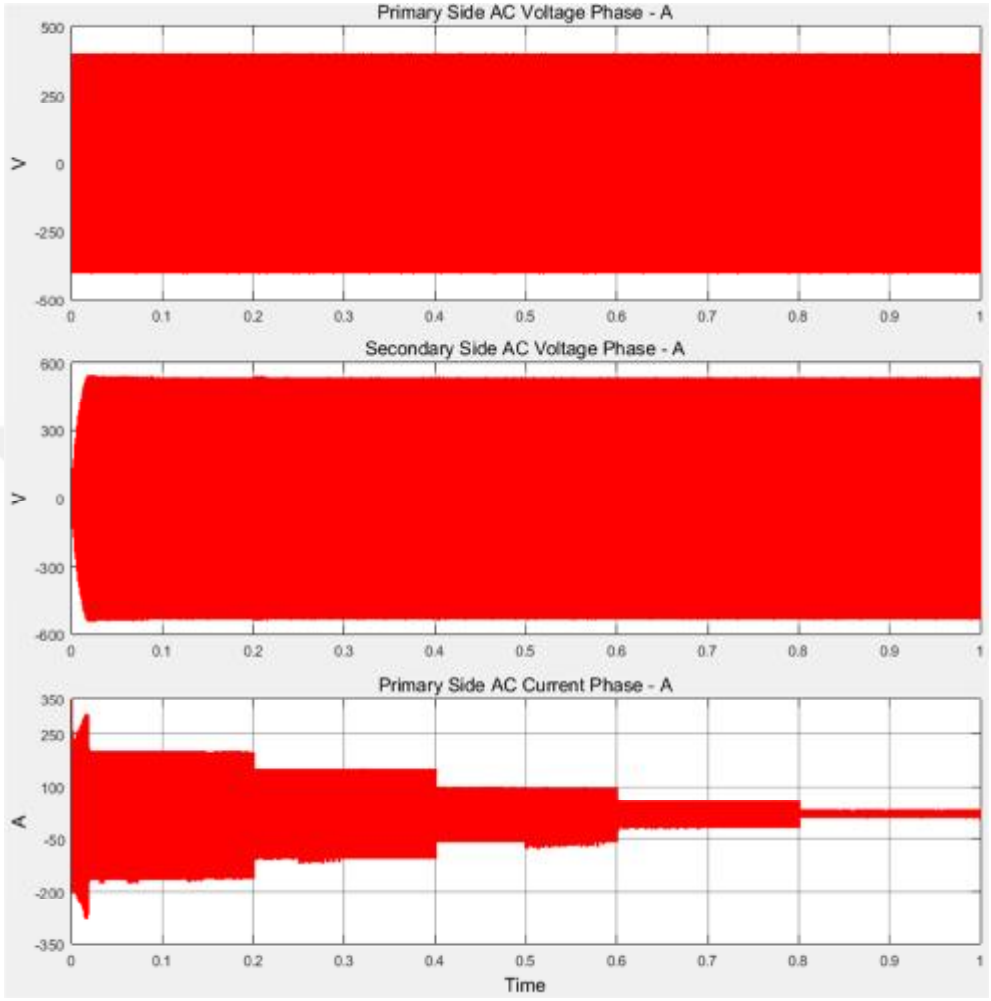

Figure 4.16. The waveforms of load changes

In addition of this case, while the system operating in %25 of full load, suddenly at t=0.2, a non-linear load is applied to the system, with 38 kW maximum power as shown in the Figure 4.17. As shown in the Figure 4.18 the phase shift is oscillates to keep the output DC voltage stable. At t=0.4 system returns %25 of full load operating condition.

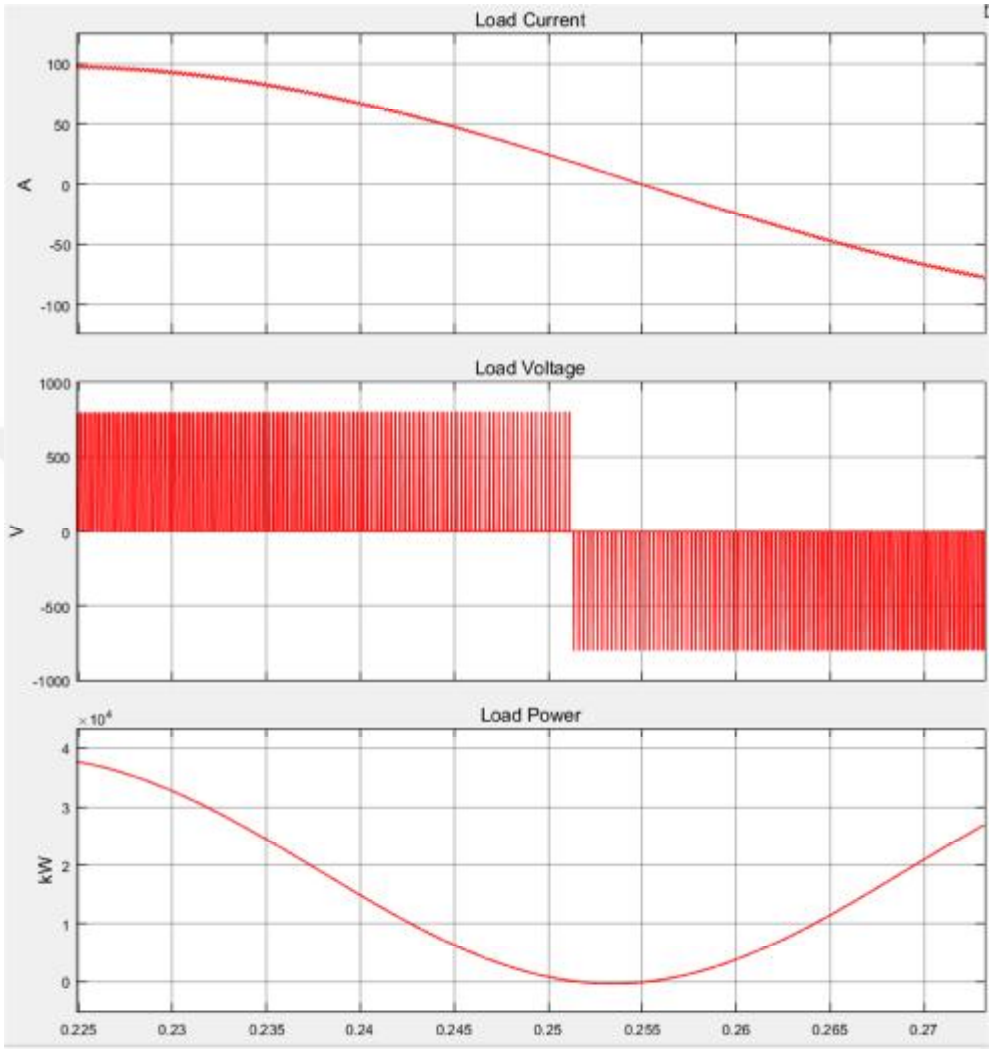

Figure 4.17. The non-linear operating waveforms

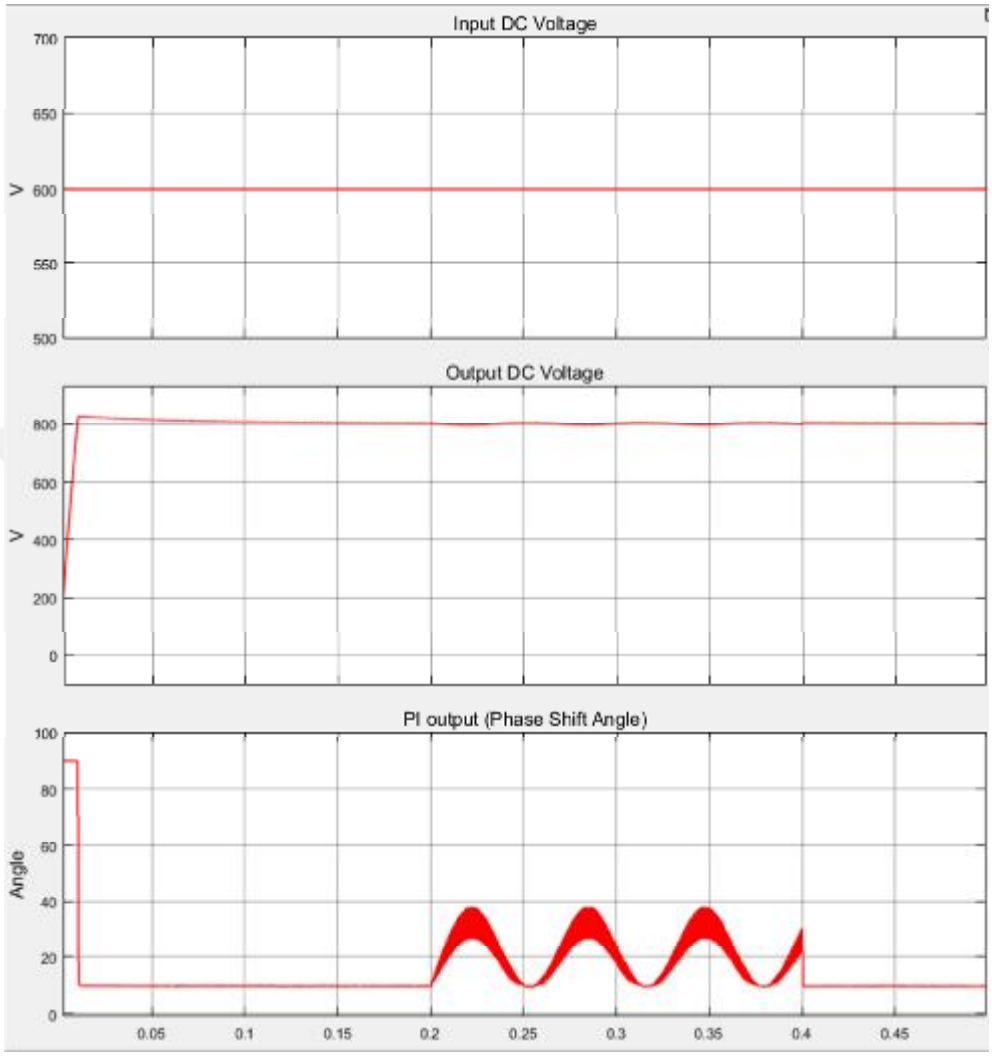

Figure 4.18. The system response of non-linear load changes

4.6. Case 5

This system is designed to provide 80 kW output power. The lower power operation conditions can also required during operation. In this case the efficiencies are analyzed in different output power conditions. Table 4.1 shows the efficiencies in different power operating conditions. Since the system designed as 80 kW, operating in lower power conditions has negative effects on efficiency.

The efficiency is basically calculated by following equation based on source voltage, source current, output voltage and output current.

$$eff = 100x\frac{(VoxIo)}{(VixIi)} \quad (4.1)$$

In this case operating with different power ranges are analyzed and the results shown in the Table 4.1. As shown, as the output power decreases, the efficiency decreases. The main reason of this situation is switching losses. In this simulation, the main components of switching losses are switching frequency and IGBT voltages and both of them are almost constant for each power range. Since the switching losses are constant for each power range, as output power decreases switching losses increases as a percentage.

Table 4.1. Efficiency analysis in different output powers

Output Power(kW)	**Output Current (A)**	**Output Voltage(V)**	**Efficiency (%)**
80.000	100	800	89,7
70.000	87,5	800	88,2
60.000	75	800	87,3
50.000	62,5	800	86,1
40.000	50	800	85,0
30.000	37,5	800	84,4
20.000	25	800	83,1
10.000	12,5	800	82,5

5. CONCLUSIONS

In this thesis, the importance and the details of the high power DC-DC converters are discussed. The dual active bridge DC-DC converters are discussed in detail and single phase and three phase DC-DC converters are compared. A three phase dual active bridge isolated bidirectional DC-DC converter is selected based on high power applications.

The system operating ranges are defined as 600 V input voltage, 800 V output voltage, 80 kW output power. The system consists of two separate converters connected with Y-Y isolation transformer with 1:1.33 turns ratio and the switching frequency is selected as 20 kHz. The 1200 V 120 A IGBTs are used as switching device for both converters since it is best option for this power and operating ranges. Converters are controlled by phase shift method and %50 fixed duty cycle is selected based on three phase controlling requirements.

The power transfer between two converters is achieved by applying phase shift between AC voltages of both sides. The key component of power transfer is total equivalent leakage inductance. This value is calculated as 29.16 µH and assumed as 20 µH based on real operating condition.

Considering some applications that has limitations on free space, a high frequency transformer is selected to provide compact design. Minimum output filter capacitors are also calculated and selected based on capacitor datasheets.

MATLAB/Simulink program is used for simulations and all component parameters are selected from datasheets to provide get real simulation results. The 12 gate signals and phase shifts are produced by a MATLAB function and power transfer direction and phase angle quantity is determined by another MATLAB function with PI controller. Dual power flow control was provided by the positive and negative phase shifts as a result of a PI controller. This PI controller compares the two quantity of set and the actual output voltages and provides a phase shift

depends on the result of comparison. Function block sample times are defined based on speed requirements of processes.

All the system requirements were considered and the design was supported with the calculation formulas.

Simulating some high power application conditions requires some considerations depending on grid and load conditions. Voltage and load changes or fluctuations and regenerative situations must be taken into account and the system must detect this changes and respond as much as quick to keep stable operation. Some cases are simulated to check and verify the system responses during non-stable conditions.

In the first case, start-up operating conditions and working principle of the circuit are analyzed. Related waveforms are also compared and checked with theoretical waveforms and all the results are similar with the theoretical forms.

In the second case, bidirectional operation of the circuit was analyzed by increasing of output DC voltage to simulate regenerative operation. In this condition negative phase shift angle is applied between two converters to transfer the power flow in opposite direction.

Although the system is designed according to 600 V input and 800 V output voltages, input voltage changes and fluctuations are always possible because of being connected to grid. These changes and fluctuations can be either in short or longer time intervals. Even these situations can affect the efficiency of the system, converter must keep the output voltage stable. In third case these conditions and system responses are analyzed. Increase, decrease and oscillation are applied to the input voltage and the results are analyzed. It is shown that system can provide the output voltage stability successfully.

Another problem in some high power applications the load conditions can always changes depends on the application types. In fourth case these conditions are analyzed by providing some load changes in different time intervals. The

results show that the system can also handle these conditions and provide stable output voltage in each situation.

Although the system is designed as 80 kW output power, the load conditions can change randomly as explained in the fourth case. In the last case this situations are analyzed and compared based on efficiency. Since the switching losses are almost same in each operating power conditions, as the power decreases the switching losses, as a percentage, increases. Thus the efficiency decreases. The results show that as the power decreases, the efficiency also decreases.

As a result, different simulation cases were analyzed by applying some changes to the input and the output sides. Input voltage changes, fluctuations, output load changes were analyzed. The system can handle these changes and keep the output DC voltage stable successfully. It is also shown that, although the system designed as 80 kW, lower power operation conditions cause lower efficiencies.

6. FUTURE WORKS

As shown in the previous chapters, power operating ranges and power requirements are very important for the system efficiency. Since the switching losses are the major effect on this kind of systems in future soft switching methods will be researched to provide efficiency in wide power range operation. Different transformer connections will also be analyzed, compared and integrated with suitable soft switching methods.

REFERENCES

Baars, N.H., Student Member, IEEE, Everts, J., Member, IEEE, Cornelis, G. E. Wijnands, and Lomonova, E.A., Senior Member, IEEE, 2016. Performance Evaluation of a Three-Phase Dual Active Bridge DC–DC Converter With Different Transformer Winding Configurations. IEEE Transactions On Power Electronics, 31(10).

Baars,N.H., Student Member, IEEE, Everts,J. Member, IEEE, Huisman, Duarte,J.L. Member, IEEE, and Lomonova,E.A., Senior Member, IEEE,2015. A 80-kW isolated dc–dc converter for railway applications. IEEE Transactions On Power Electronics, 30(12):pp.6639-6647

Barnes M., 2003. Practical variable speed drives and power electronics, pp.287

Cheung, P.,2017. PID controller, Imperial College , Lecture 17, pp.12

Chiu, H.J., and Lin, L.W.,2006. A bidirectional dc-dc converter for fuel cell electric vehicle driving system. IEEE Trans. Power Electron., 21(4):pp.950–958

De Doncker, R. W., Divan, D. M. and Kheraluwala, M. H.,1991. A three-phase soft-switched high power density dc-to-dc converter for high power applications IEEE Trans. Industry Applications, 27(1):pp.63-73.

Dutta, S., 2014. Controls and applications of the dual active bridge dc to dc converter for solid state transformer applications and integration of multiple renewable energy sources. North Carolina State University Phd Thesis, UMI Number: 3647615 pp.185

George, K., 2015. Design and control of a bidirectional dual active bridge dc-dc converter to interface solar, battery storage, and grid-tied inverters. Arkansas University Electrical Engineering Undergraduate Honors Theses, Paper 45, pp:85.

Hoek, H.V., Student Member, IEEE, Neubert,M., Student Member, IEEE, and Doncker,R.W.D, Fellow, IEEE,2013. Enhanced Modulation Strategy for a Three-Phase Dual Active Bridge—Boosting Efficiency of an Electric Vehicle Converter. IEEE Transactions On Power Electronics, 28(12):pp.5499-5507

Inoue,S., Member, IEEE, and Akagi,H., Fellow, IEEE, 2007. A bidirectional dc-dc converter for an energy storage system with galvanic isolation. IEEE Transactions On Power Electronics,22(6):pp.2299-2306

Jain, M. Daniele, M. and Jain, P. K.,2000 A bidirectional dc-dc converter topology for low power application. IEEE Trans. Power Electron., 15(4):pp.595–606.

Kheraluwala, M. H., 1991. High-power high-frequency DC-to-DC converters. ProQuest Dissertations & Theses Global, 9126422, pp.268

Kheraluwala, M.H., Gascoigne, R. W., Member, IEEE, Divan, D.M., Member, IEEE and Baumann, E.D., 1992. Performance characterization of a high-power dual active bridge dc-to-dc converter. IEEE Transactions On Industry Applications, 28(6).

Kinjo, T., Senjyu, T., Urasaki, N., and Fujita, H.,2006. Output levelling of renewable energy by electric double layer capacitor applied for energy storage system. IEEE Trans. Energy Convers., 21(1):pp.221–227.

Krismer, F., 2010. Modeling and optimization of bidirectional dual active bridge dc–dc converter topologies. A dissertation submitted to Eth Zurich Diss. Eth No. 19177, pp.443

Krismer,F., Round,S., Kolar J.W., Performance optimization of a high current dual active bridge with a wide operating voltage range.

Ribeiro, P.F., Johnson B. K., Crow, M. L., Arsoy A., and Liu, Y., 2001. Energy storage systems for advanced power applications. Proc. IEEE, 89(12):pp.1744–1756.

Schibli, N.,2000. Symmetrical multilevel converters with two quadrant dc-dc feeding. Ecole Polytechnique Federale De Lausanne,these no:2220 pp.285

Segaran, D., Holmes, D. G. and McGrath, B. P., 2008. Comparative analysis of single and three-phase dual active bridge bidirectional dc-dc converters. In Proc. Power Eng. Conf., Dec. 2008, pp. 1–6

Segaran, D., Holmes, D.G., McGrath, B.P.,2008. Comparative analysis of single and three-phase dual active bridge bidirectional dc-dc converters. 2008 Australasian Universities Power Engineering Conference (AUPEC'08) Paper P-212.

Semikron, 2007. "AN1114". https://www.microchip.com. Last Access Date: October 2014.

Tan, L.M.L., Member, IEEE, Abe,T. and Akagi,H., Fellow, IEEE,2012. Design and performance of a bidirectional isolated dc–dc converter for a battery energy storage system. IEEE Transactions On Power Electronics, 27(3):pp.1237-1248

Wang Z.,2012. Interleaved multi-phase isolated bidirectional dc-dc converter and its extension. The Florida State University College of Engineering, Phd Thesis, UMI Number: 3539865, pp.105

Yilmaz M. Member, IEEE, and Philip T. Krein, Fellow, IEEE 2013. Review of Battery Chargertopologies, Charging ,Power Levels, And Infrastructure For Plug-in Electic and Hybrid Vehicles IEEE Transactions on Power Electronics , 28 (5):pp 2151-2169

Zhang, J., 2008, Bidirectional dc-dc power converter design optimization, modeling and control. Dissertation submitted to the faculty of the Virginia Polytechnic Institute, UMI Number: DP19255

Zhao,B., Student Member, IEEE, Song,Q., Member, IEEE, Liu,W., Member, IEEE, and Sun, Y., 2014. Overview of dual-active-bridge isolated bidirectional dc–dc converter for high-frequency-link power-conversion system. IEEE Transactions On Power Electronics, 29(8).

BIOGRAPHY

Ferdi Ekinoğlu was born in Abha, Saudi Arabia in 1987. He received his B.Sc. Electrical and Electronics Engineering Department from Mersin University, Mersin, Turkey, in 2010. He has been working as Technical Services Engineer in Siemens since 2012 and studying in Cukurova University, Adana on Power Electronics as MSc. since 2013. His research interests include power electronics, drive systems and electric vehicles.

APPENDIX

APPENDIX A: TECHNICAL SPECIFICATIONS OF IGBT

Table A.1 Technical Specifications of SK120GB12F4T (Semikron, 2016)

SK 120 GB 12F4 T

SEMITOP® 3

IGBT module

SK 120 GB 12F4 T

Target Data

Features

- Compact design
- One screw mounting module
- Optimum heat transfer and isolation through AlN direct copper bonding (DBC)
- Trench4 Fast IGBT technology
- CAL4F diode technology
- Integrated NTC temperature sensor
- UL recognized, file no. E 63 532

Typical Applications*

- Switching (not for linear use)
- Inverter
- Switched mode power supplies
- UPS

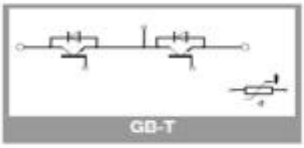

GB-T

Absolute Maximum Ratings

Symbol	Conditions		Values	Unit
Inverter - IGBT				
V_{CES}	T_j = 25 °C		1200	V
I_C	T_j = 175 °C	T_s = 25 °C	174	A
		T_s = 70 °C	143	A
I_{Cnom}			120	A
I_{CRM}	I_{CRM} = 3 x I_{Cnom}		360	A
V_{GES}			-20 ... 20	V
t_{psc}	V_{CC} = 600 V V_{GE} ≤ 15 V V_{CES} ≤ 1200 V	T_j = 150 °C	10	µs
T_j			-40 ... 175	°C
Inverse - Diode				
I_F	T_j = 175 °C	T_s = 25 °C	29	A
		T_s = 70 °C	24	A
I_{Fnom}			15	A
I_{FRM}	I_{FRM} = 3 x I_{Fnom}		45	A
I_{FSM}	10 ms, sin 180°, T_j = 150 °C		65	A
T_j			-40 ... 175	°C
Module				
$I_{t(RMS)}$	-			A
T_{stg}			-40 ... 125	°C
V_{isol}	AC, sinusoidal, t = 1 min		2500	V

Characteristics

Symbol	Conditions		min.	typ.	max.	Unit
Inverter - IGBT						
$V_{CE(sat)}$	I_C = 120 A V_{GE} = 15 V chiplevel	T_j = 25 °C		2.05	2.40	V
		T_j = 150 °C		2.50	2.85	V
V_{CE0}	chiplevel	T_j = 25 °C		0.80	0.90	V
		T_j = 150 °C		0.70	0.80	V
r_{CE}	V_{GE} = 15 V chiplevel	T_j = 25 °C		10	13	mΩ
		T_j = 150 °C		15	17	mΩ
$V_{GE(th)}$	V_{GE} = V_{CE}, I_C = 4.5 mA		5.2	5.8	6.4	V
I_{CES}	V_{GE} = 0 V V_{CE} = 1200 V	T_j = 25 °C			1.6	mA
						mA
C_{ies}	V_{CE} = 25 V V_{GE} = 0 V	f = 1 MHz		6.9		nF
C_{oes}		f = 1 MHz		0.555		nF
C_{res}		f = 1 MHz		0.405		nF
Q_G	- 15 V ... + 15 V			430		nC
R_{Cint}	T_j = 25 °C			2.7		Ω
$t_{d(on)}$	V_{CC} = 600 V	T_j = 150 °C		156		ns
t_r	I_C = 120 A	T_j = 150 °C		51		ns
E_{on}	$R_{G\,on}$ = 2.2 Ω	T_j = 150 °C		8.8		mJ
$t_{d(off)}$	$R_{G\,off}$ = 2.2 Ω di/dt_{on} = 2364 A/µs	T_j = 150 °C		346		ns
t_f	di/dt_{off} = 2264 A/µs	T_j = 150 °C		42		ns
E_{off}	V_{GE} = +15/-15 V	T_j = 150 °C		7.47		mJ
$R_{th(j-s)}$	per IGBT			0.22	0.25	K/W

APPENDIX B: TECHNICAL SPECIFICATIONS OF CAPACITOR

Table B.2 Technical Specifications of MKP DC B2562 (Epcos, 2016)

$V_{R\,DC}$ = 700 V DC / V_{TT} = 1050 V DC, 10 s / V_{TC} = 4000 V AC, 10 s

C_R µF	I_{MAX}[1] A	I_s kA	$\hat{I}$ kA	ESR[2] mΩ	L_{self} nH	R_{TH} K/W	D mm	H_C mm	H_T mm	Weight kg	Fig.	Ordering code
280	55	12.1	4.0	1.2	≤ 40	4.0	85	70	76	0.45	1	B25620B0287K701
500	60	13.5	4.5	1.3	≤ 40	3.0	90	95	124	0.73	3	B25623B0507K704
560	80	24.2	8.0	1.1	≤ 40	2.9	116	70	76	0.88	4	B25620B0567K703
620	55	12.1	4.0	1.9	≤ 40	2.9	85	120	126	0.71	1	B25620B0627K701
700	55	12.1	4.0	2.0	≤40	2.8	85	132	138	0.87	1	B25620B0707K701
780	65	13.4	4.5	1.9	≤ 40	2.5	90	132	161	1.00	3	B25623B0787K704
900	80	24.3	8.0	1.2	≤ 40	2.3	116	95	101	1.13	4	B25620B0907K703
1240	80	24.3	8.1	1.3	≤ 40	2.2	116	120	126	1.40	4	B25620B0128K743
1400	80	24.1	8.0	1.6	≤ 40	2.1	116	132	138	1.55	4	B25620B0148K703

$V_{R\,DC}$ = 900 V DC / V_{TT} = 1350V DC, 10 s / V_{TC} = 4000 V AC, 10 s

C_R µF	I_{MAX}[1] A	I_s kA	$\hat{I}$ kA	ESR[2] mΩ	L_{self} nH	R_{TH} K/W	D mm	H_C mm	H_T mm	Weight kg	Fig.	Ordering code
220	50	10.8	3.6	1.3	≤ 40	4.0	85	70	76	0.45	1	B25620B0227K881
220	50	10.8	3.6	1.3	≤ 40	4.0	85	74	76	0.48	2	B25620C0227K881
350	50	10.7	3.6	1.5	≤ 40	3.3	85	95	101	0.58	1	B25620B0357K881
350	50	10.7	3.6	1.5	≤ 40	3.3	85	99	101	0.61	2	B25620C0357K881
420	60	11.9	4.0	1.4	≤ 40	3.0	90	95	124	0.73	3	B25623B0427K904
440	65	21.7	7.2	0.8	≤ 40	2.9	116	70	76	0.88	4	B25620B0447K883
480	55	10.8	3.6	2.0	≤ 40	2.9	85	120	126	0.71	1	B25620B0487K881
480	55	10.8	3.6	2.0	≤ 40	2.9	85	124	126	0.74	2	B25620C0487K881
550	50	11	3.7	2.8	≤ 40	2.8	85	132	138	0.87	1	B25620B0557K881
550	50	11	3.7	2.8	≤ 40	2.8	85	136	138	0.9	2	B25620C0557K881
580	62	11.9	4.0	1.8	≤ 40	2.8	90	120	149	0.9	3	B25623B0587K904
650	62	11.8	3.9	2.0	≤ 40	2.5	90	132	161	1	3	B25623B0657K904
700	70	21.5	7.1	1.3	≤ 40	2.3	116	95	101	1.13	4	B25620B0707K883
730	62	11.8	3.9	2.8	≤ 60	2.3	90	145	174	1.2	3	B25623B0737K904
750	75	23.1	7.7	1.1	≤ 60	2.1	85	173	179	1.1	1	B25620B0757K881
750	75	23.1	7.7	1.1	≤ 60	2.1	85	177	179	1.13	2	B25620C0757K881
830	75	23.5	7.8	1.5	≤ 60	2.0	90	173	202	1.3	3	B25623B0837K904
970	75	21.7	7.2	1.9	≤ 40	2.2	116	120	126	1.4	4	B25620B0977K883
1100	80	21.7	7.2	1.4	≤ 40	2.1	116	132	138	1.55	4	B25620B0118K883
1500	100	43	15.4	1.1	≤ 60	2.0	116	173	179	1.945	4	B25620B0158K883
1500	100	43	15.4	1.1	≤ 60	2.0	116	177	179	1.945	5	B25620C0158K883

APPENDIX C: THE MATLAB FUNCTION CODES

1. The Gate Driver Codes

```
function [gA1,gA2,gA3,gA4,gA5,gA6,gB1,gB2,gB3,gB4,gB5,gB6,u] =
GateGen(tri,Ref1)
%#codegen

if (tri>=0) && (tri<1/2)
   gA1=1;
   gA4=0;
else
   gA1=0;
   gA4=1;
end
if (tri>=2/6) && (tri<5/6)
   gA3=1;
   gA6=0;
else
   gA3=0;
   gA6=1;
end
if (tri>=4/6) || (tri<1/6)
   gA5=1;
   gA2=0;
else
   gA5=0;
   gA2=1;
end
```

```
if (Ref1<0)
   if (tri>=(1+Ref1)) || (tri<(1/2+Ref1))
      gB1=1;
      gB4=0;
   else
      gB1=0;
      gB4=1;
   end
   if (tri>=(2/6+Ref1)) && (tri<(5/6+Ref1))
      gB3=1;
      gB6=0;
   else
      gB3=0;
      gB6=1;
   end
   if (Ref1<-1/6)
      if (tri>=(4/6+Ref1)) && (tri<(1+1/6+Ref1))
         gB5=1;
         gB2=0;
      else
         gB5=0;
         gB2=1;
      end
   else
      if (tri>=(4/6+Ref1)) || (tri<(1/6+Ref1))
         gB5=1;
         gB2=0;
      else
         gB5=0;
```

```
            gB2=1;
        end
    end
else
    if (tri>=Ref1) && (tri<(1/2+Ref1))
        gB1=1;
        gB4=0;
    else
        gB1=0;
        gB4=1;
    end
    if (Ref1>1/6)
        if (tri>=(2/6+Ref1)) || (tri<(Ref1-1/6))
            gB3=1;
            gB6=0;
        else
            gB3=0;
            gB6=1;
        end
    else
        if (tri>=(2/6+Ref1)) && (tri<(5/6+Ref1))
            gB3=1;
            gB6=0;
        else
            gB3=0;
            gB6=1;
        end
    end
    if (tri>=(4/6+Ref1)) || (tri<(1/6+Ref1))
```

```
        gB5=1;
        gB2=0;
    else
        gB5=0;
        gB2=1;
    end
end

 u=tri;

end
```

2. PI Controller Codes

```
function [Ref,Idc1, PIdc1]  = Control(Vout, VdcRef)
%#codegen
global VdcErr;
global Pdc;
global Idc;
global PIdc;

Kp=3;
Ki=50;

Ts=50e-6;

LimPIp=90;
LimPIn=-90;
```

```
VdcErr = VdcRef - Vout;
Pdc = Kp*VdcErr;
Idc = Idc + Ki*Ts*VdcErr;
PIdc = Pdc + Idc;
if PIdc > LimPIp
   PIdc = LimPIp;
   Idc = LimPIp;
end
if PIdc < LimPIn
   PIdc = LimPIn;
   Idc = LimPIn;
end

Ref = (PIdc/360);
Idc1=Idc;
PIdc1=PIdc;


End
```

2. Variable Load Codes

```
function [o1,o2,o3,o4] = fcn(t)
s1=0;
s2=0;
s3=0;
s4=0;
if(t<=2.1)
   s1 = 1;
   s2 = 0;
```

```
    s3 = 0;
    s4 = 0;
end
if(t>=2.1&&t<=2.4)
    s1 = 0;
    s2 = 1;
    s3 = 0;
    s4 = 0;
end
if(t>=2.4&&t<=2.7)
    s1 = 1;
    s2 = 0;
    s3 = 0;
    s4 = 0;
end
if(t>=2.7&&t<=3)
    s1 = 0;
    s2 = 1;
    s3 = 0;
    s4 = 0;
end
if(t>=3&&t<=3.3)
    s1 = 1;
    s2 = 0;
    s3 = 0;
    s4 = 0;
end
if(t>=3.3&&t<=3.6)
    s1 = 0;
```

```
    s2 = 0;
    s3 = 1;
    s4 = 0;
end
if(t>=3.6&&t<=3.9)
    s1 = 1;
    s2 = 0;
    s3 = 0;
    s4 = 0;
end
if(t>=3.9&&t<=4.2)
    s1 = 0;
    s2 = 0;
    s3 = 0;
    s4 = 1;
end
if(t>=4.2)
    s1 = 1;
    s2 = 0;
    s3 = 0;
    s4 = 0;
end

o1=s1;
o2=s2;
o3=s3;
o4=s4;
end
```

4. Variable Input Voltage Codes

```
function s  = fcn(t)
s=800;
if(t<=0.3)
   s=600;
end
if(t>=0.3&&t<=0.6)
   s=660;
end
if(t>=0.6&&t<=0.9)
   s=600;
end
if(t>=0.9&&t<=1.2)
   s=540;
end
if(t>=1.2&&t<=1.5)
   s=600;
end
if(t>=1.5&&t<=1.8)
   s=600+60*sin(2*pi*20*t);
end
if(t>=1.8)
   s=600;
end

end
```